

Self-Assembled Monolayers (SAMs)

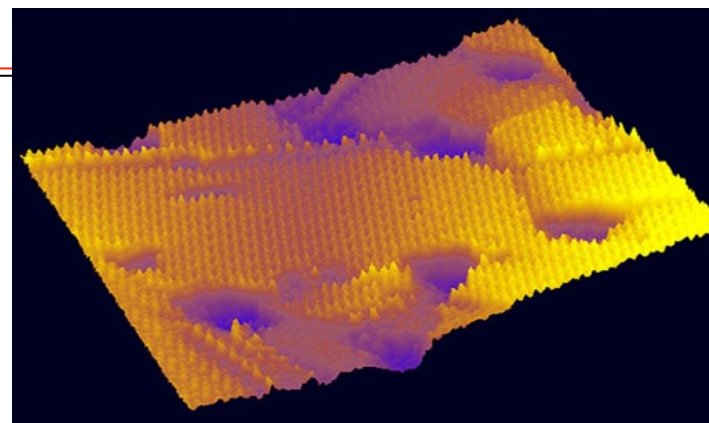
A. Ulman *Chem. Rev.* **1996**, *96*, 1533-1554.

J. C. Love, L. A. Estroff, J. K. Kriebel, R. G. Nuzzo, G. M. Whitesides
Chem. Rev. **2005**, *105*, 1103-1169.

nanostructures are “all surface”

$$V \propto l^3$$

$$S \propto l^2$$



STM Image of a SAM

- atoms or molecules at the surface of a material experience a different environment from those in the bulk and thus have different free energies, electronic states, reactivities, mobilities, and structures.
- the physical properties of nanostructures depend to a much greater extent on their surface and interfacial environment than do bulk material.

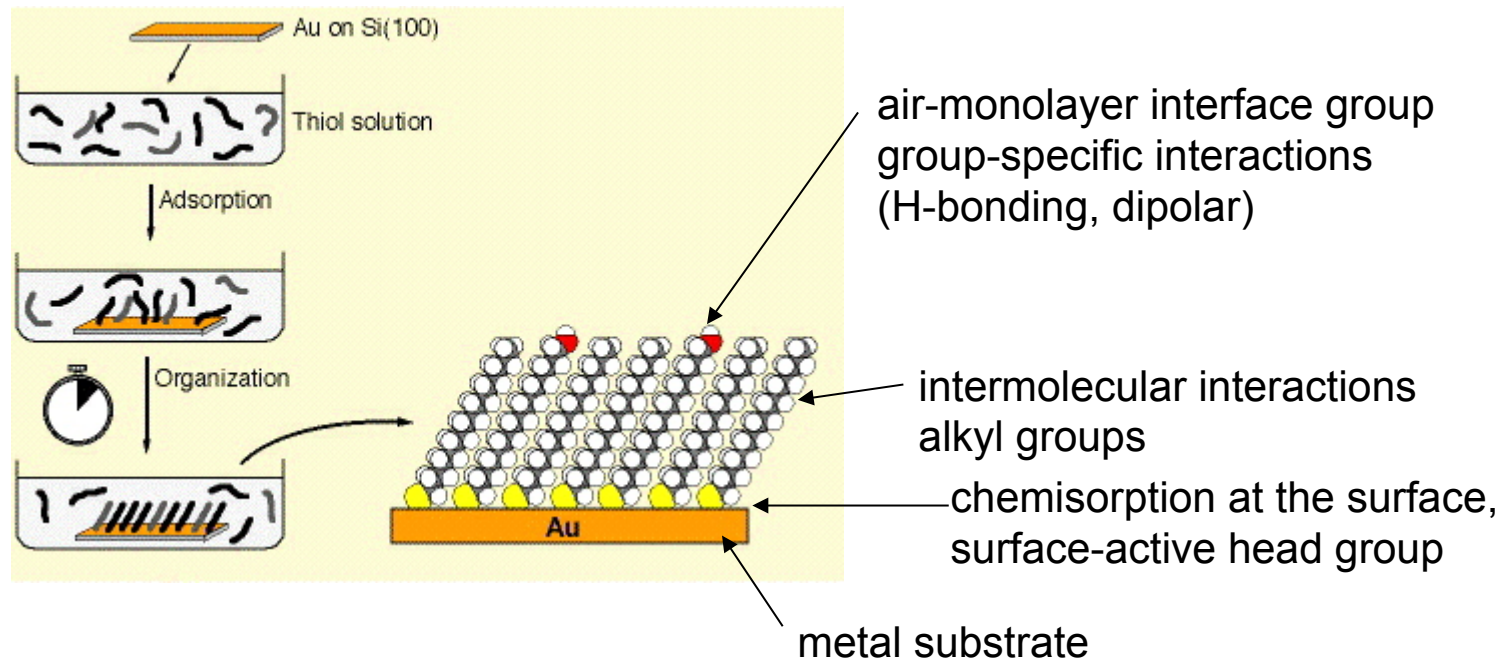
2D-SAMs

Table 1. Combinations of Headgroups and Substrates Used in Forming SAMs on Metals, Oxides, and Semiconductors

Ligand	Substrates	Morphology of Substrate		Ligand	Substrates	Morphology of Substrate				
		Thin Films or Bulk Material	Nanoparticles or Other Nanostructures			Thin Films or Bulk Material	Nanoparticles or Other Nanostructures			
ROH	Fe ₂ O ₃		35	RSSR ⁺	Ag	89	90			
	Si-H	36			Au	20	90-92			
	Si	37			CdS		61			
RCOO-RCOOH	α -Al ₂ O ₃	38,39			Pd	30				
	Fe ₂ O ₃		40		Au	93				
	Ni		41,42							
	Ti/TiO ₂	43								
RCOO-OOCR	Si(111):H	44		RCSSH	Au	94				
	Si(100):H			CdSe		95				
Ene-diol	Fe ₂ O ₃		45	RS ₂ O ₂ /Na ⁺	Au	96	98			
RNH ₂	FeS ₂	46			Cu	97				
	Mica	47			RSell	Ag	99			
	Stainless Steel 316L	48		Au		100,101				
	YBa ₂ Cu ₃ O _{7-δ}	49		CdS			60			
	CdSe		50	CdSe		102				
RC=N	Ag	51		RSeSeR ⁺	Au	101				
	Au									
R-NiN ⁺ (BF ₄ ⁻)	GaAs(100)	52		R ₂ P	Au		103			
	Pd	52			FeS ₂		104			
	Si(111):H	52			CdS	46	104			
RSH	Ag	26	53,54		CdSe		104			
	Ag ₂ Ni ₃	55			CdTe		104			
	AgS		56	R ₂ I=O	Cu		106, 106			
	Au	26	57		CdS		104			
	AuAg		58		CdSe		104			
	AuCu		58		CdTe		104			
	Au ₂ Pd _{1-x}		58		RPO ₂ ²⁻ /RP(O)(OH) ₂	Al	107			
	CdTe		59	Al-OH		108				
	CdSe		60	Cu ₂ (PO ₃ CO ₃) ₂ (OH) ₂		109				
	CdS		61,62	GaAs		110				
	Cu	26	58	GaN		110				
	FePt		63-66	Indium tin oxide		111				
	GaAs	67		(ITO)						
	Ge	68		Mica		112				
	Hg	69-71		TiO ₂		113,114				
	HgTe		72	ZnO		114,115				
	InP	73		CdSe			116-118			
	Ir		74	CdTe			118,119			
	Ni	75		RPO ₄ ³⁻		Al ₂ O ₃	120			
	PbS		76-78			Nb ₂ O ₅	120			
	Pd	30	74,79			Ta ₂ O ₅	121			
	PdAg		58		TiO ₂	120,122				
	Pt	32	80		RN=C	Pt	123	124		
	Ru		81	RHC-CH ₂		Si	37			
	Stainless Steel 316L	48				RC=CH	Si(111):H	125		
	YBa ₂ Cu ₃ O _{7-δ}	82					RSiX ₃ X = H, Cl OCH ₂ CH ₃	HfO ₂	126	
	Zn	83							ITO	127
ZnSe	84		PtO		128					
ZnS		85	TiO ₂	113,126,129						
RSAc	Au	86		ZnO	126,129					
	Au		87							
RSSR ⁺	Au	88								

2D-SAMs

Self-assembled monolayers are formed by simply immersing a substrate into a solution of the surface-active material. The driving force for the spontaneous formation of 2D assembly includes chemical bond formation of molecules with the surface and intermolecular interactions.



piranha solution: 3:1 concentrated H_2SO_4 : 30% H_2O_2

acqua regia solution: 3:1 $\text{HCl}:\text{HNO}_3$

2D-SAMs

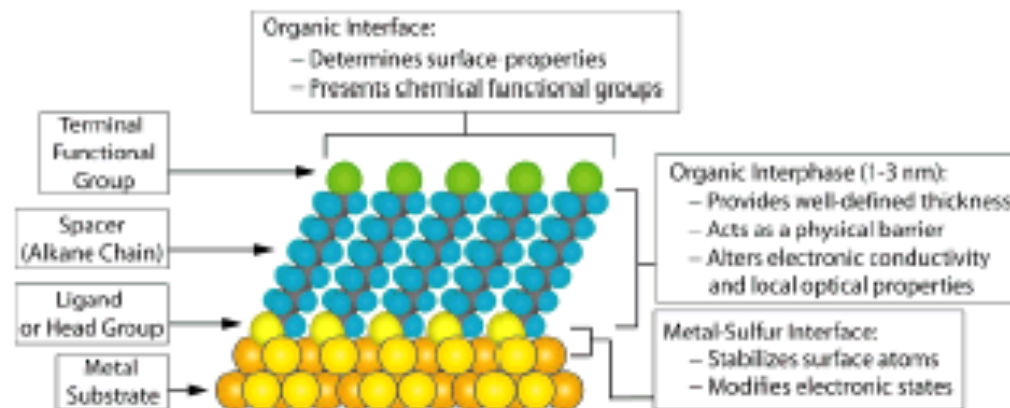
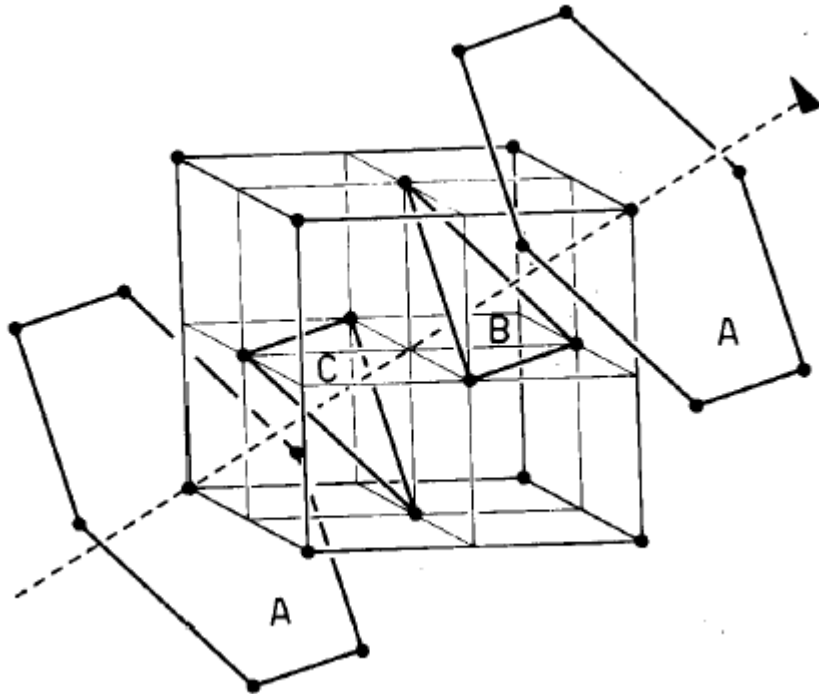


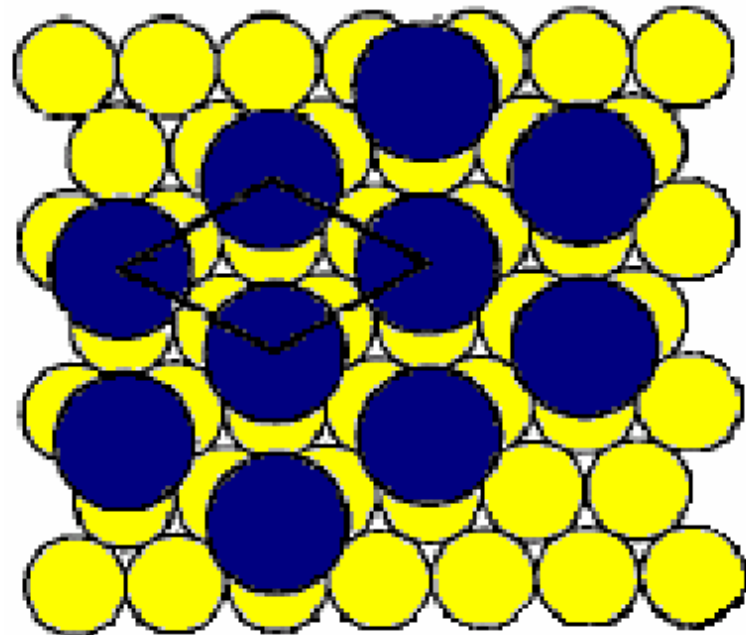
Figure 1. Schematic diagram of an ideal, single-crystalline SAM of alkanethiolates supported on a gold surface with a (111) texture. The anatomy and characteristics of the SAM are highlighted.

2D-SAMs

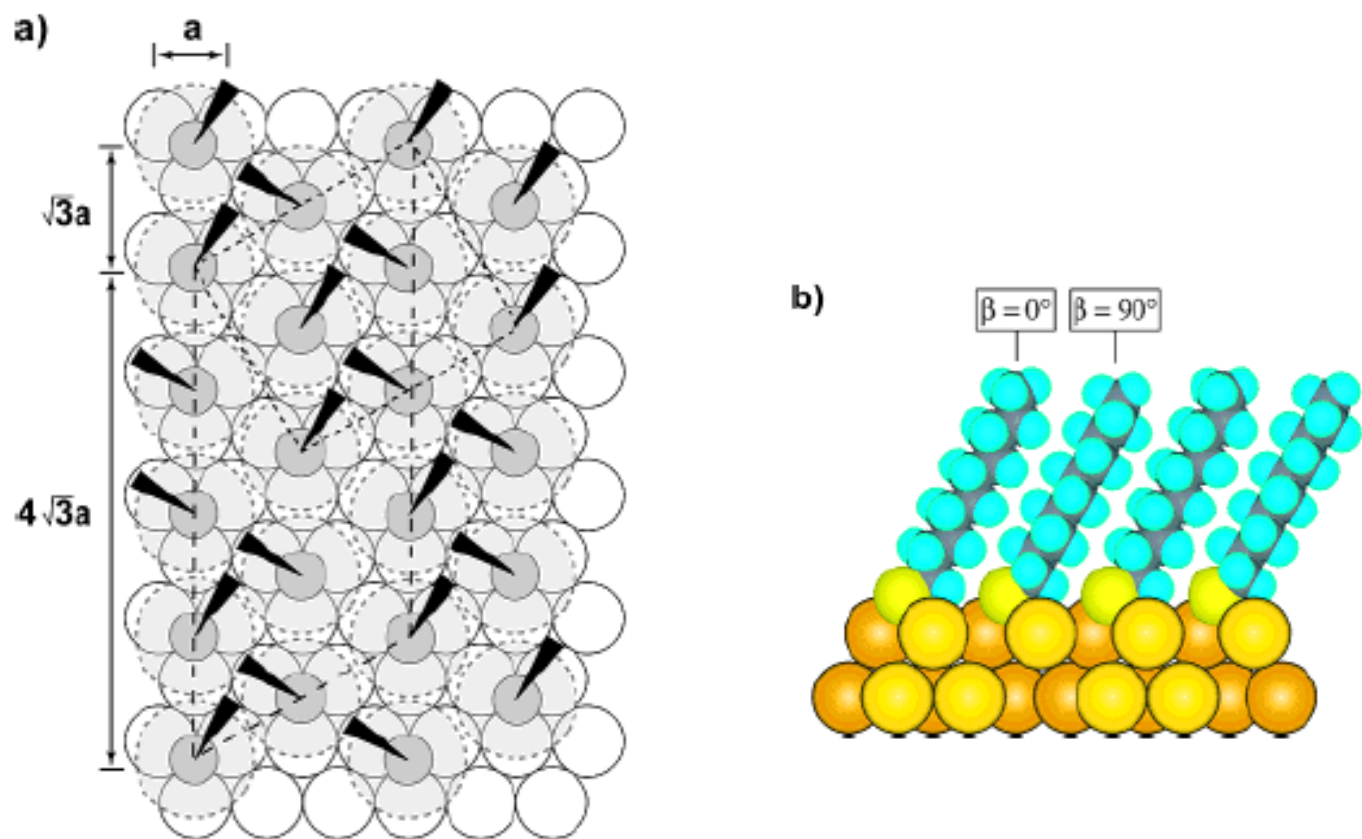
Structure of closed packed Au



$$\left(\sqrt{3} \times \sqrt{3}\right) R30$$



Au (111)



Schematic diagram depicting the arrangement of decanethiolates on Au(111) lattice when maximum coverage of the thiolates is attained. (a) Structural model of the commensurate adlayer formed by thiols on the gold lattice. The arrangement shown is a $(\sqrt{3} \times \sqrt{3})R30^\circ$ structure where the sulfur atoms (dark gray circles) are positioned in the 3-fold hollows of the gold lattice (white circles, $a = 2.88 \text{ \AA}$). The light gray circles with the dashed lines indicate the approximate projected surface area occupied by each alkane chain; the dark wedges indicate the projection of the CCC plane of the alkane chain onto the surface. Note the alternating orientation of the alkane chains defines a $c(4 \times 2)$ superlattice structure. The formal $c(4 \times 2)$ unit cell is marked (long dashes); an equivalent $2\sqrt{3} \times 3$ unit cell is marked by lines with short dashes. The alkane chains tilt in the direction of their next-nearest

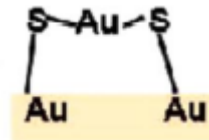
Structure of a CH₃S Monolayer on Au(111) Solved by the Interplay between Molecular Dynamics Calculations and Diffraction Measurements

R. Mazzarello,^{1,2} A. Cossaro,³ A. Verdini,³ R. Rousseau,¹ L. Casalis,⁴ M. F. Danisman,⁵ L. Floreano,³ S. Scandolo,²
A. Morgante,^{3,6} and G. Scoles^{1,4,5}

PRL 98, 016102 (2007)

Calcoli Ab-Initio DFT-based MD dimostrano che:

1. Sono stabili strutture in cui un singolo atomo di oro coordina due atomi di zolfo (motivo RS-Au-RS)
Stabilizzate dalla presenza di ADATOM



2. Sono stabili strutture a ponte (Au-S-Au)
Stabilizzate dalla presenza di VACANZE

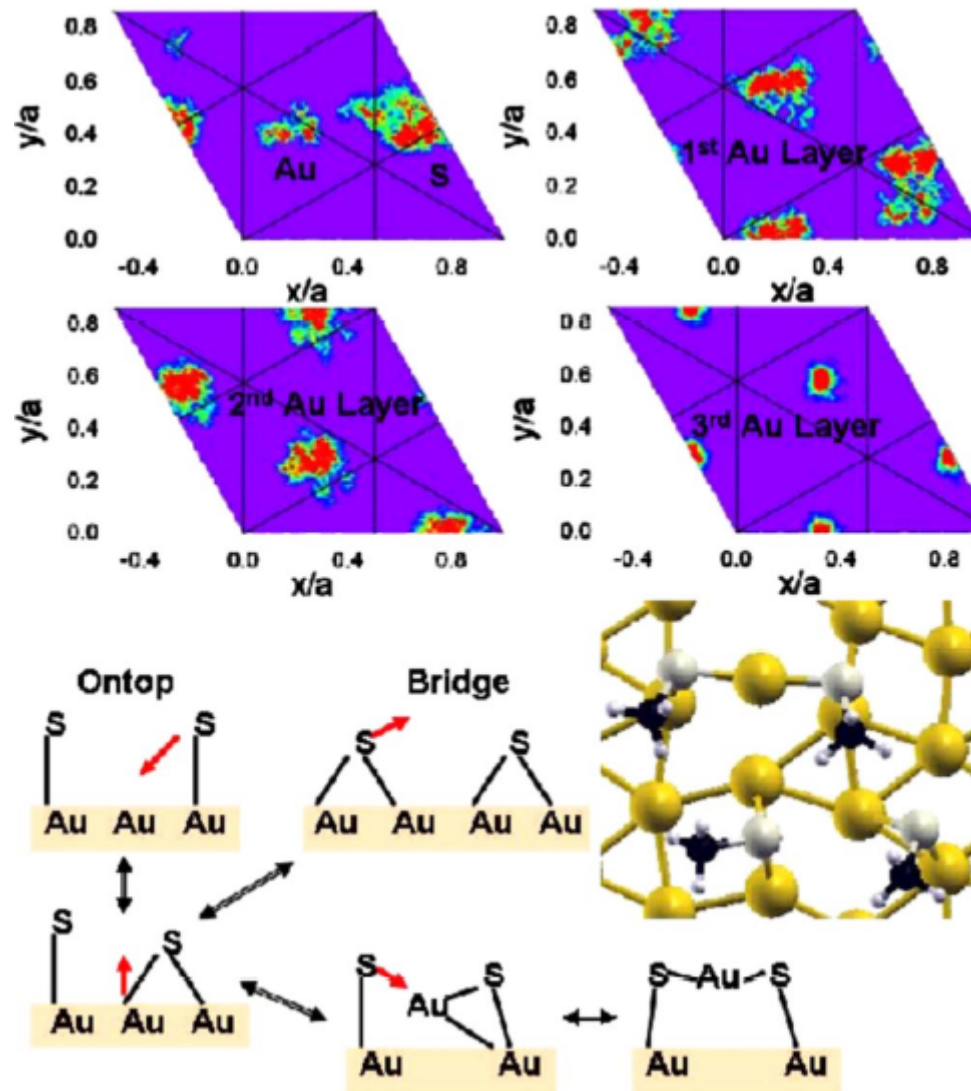


sperimentalmente: photoelectron diffraction (PED) 250-630 eV
grazing incidence x-ray diffraction (GXRD) 7000 eV, 0.5° grazing angle

Structure of a CH₃S Monolayer on Au(111) Solved by the Interplay between Molecular Dynamics Calculations and Diffraction Measurements

R. Mazzarello,^{1,2} A. Cossaro,³ A. Verdini,³ R. Rousseau,¹ L. Casalis,⁴ M.F. Danisman,⁵ L. Floreano,³ S. Scandolo,²
A. Morgante,^{3,6} and G. Scoles^{1,4,5}

PRL 98, 016102 (2007)



X-ray Diffraction and Computation Yield the Structure of Alkanethiols on Gold(111)

A. Cossaro,¹ R. Mazzarello,² R. Rousseau,^{2*} L. Casalis,³ A. Verdini,¹ A. Kohlmeier,⁴
L. Floreano,¹ S. Scandolo,⁵ A. Morgante,^{1,6†} M. L. Klein,⁴ G. Scoles^{2,3,7}

15 AUGUST 2008 VOL 321 SCIENCE 943

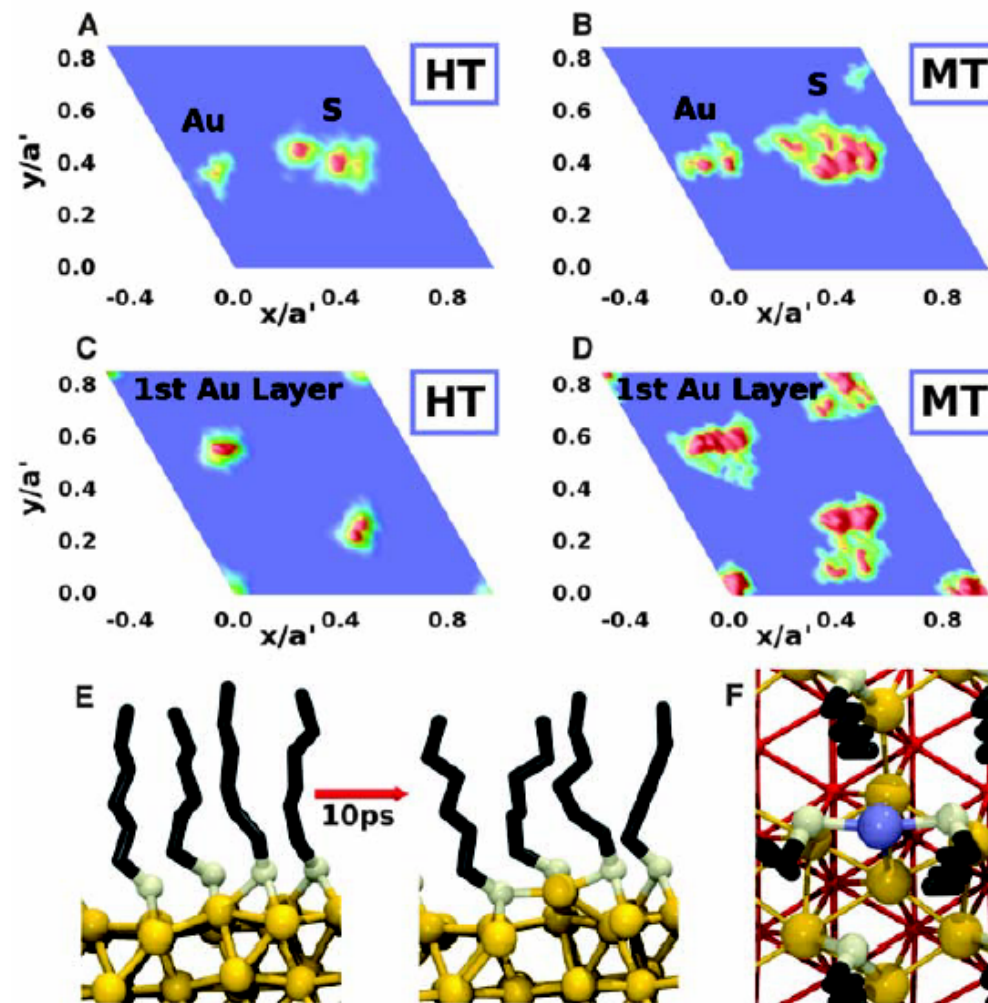
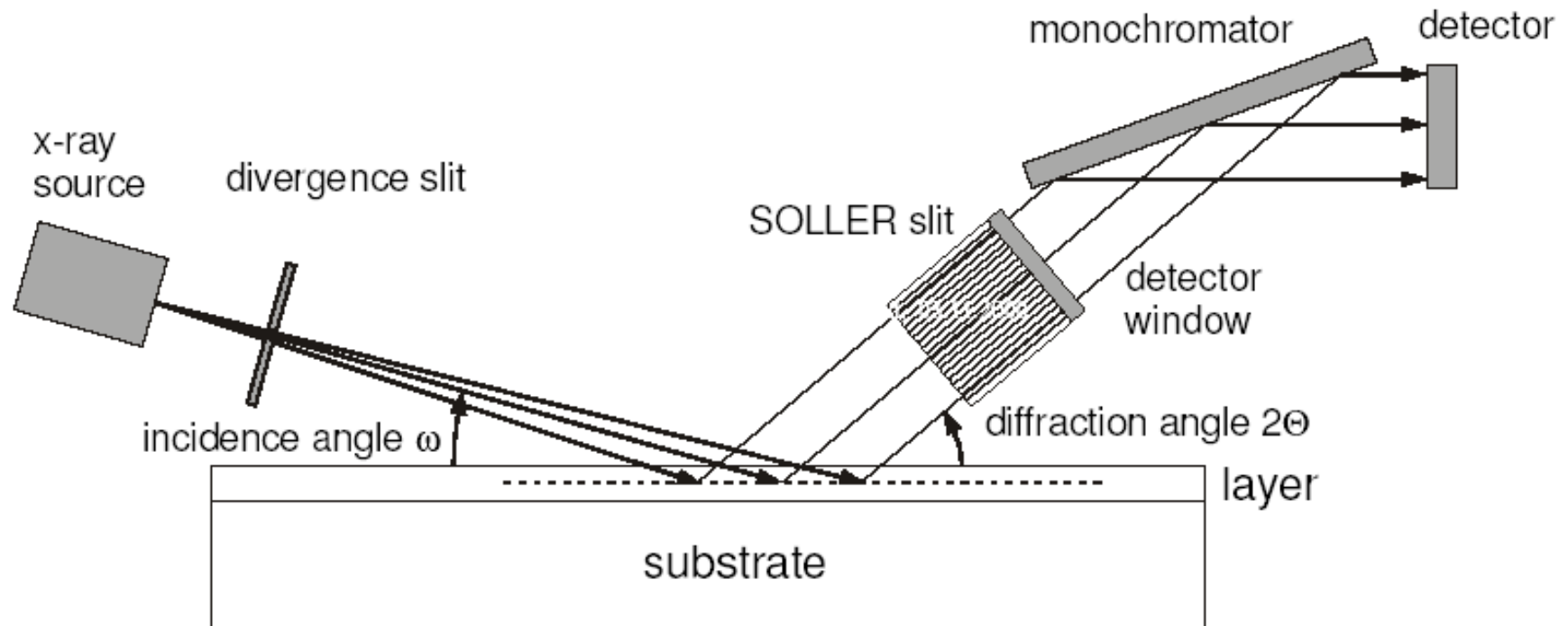


Fig. 1. Top view of the Au(111) surface and selected MD results.

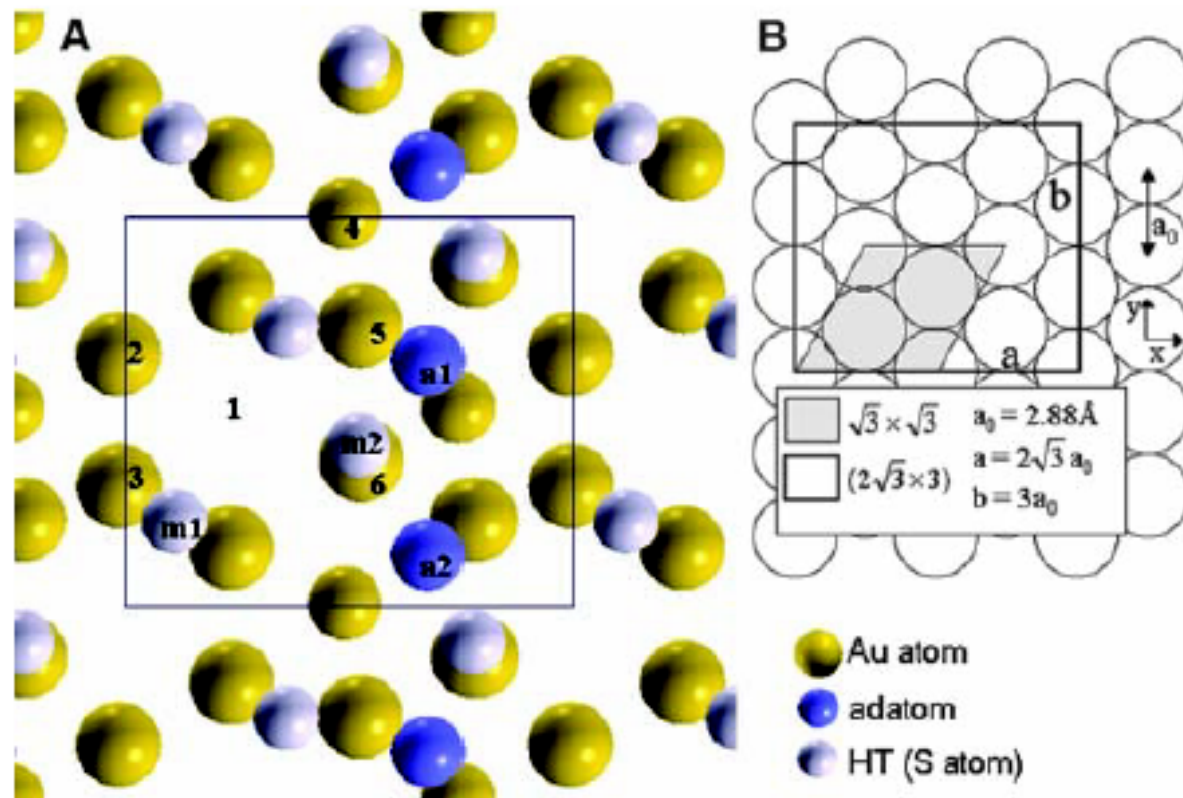
GIXRD

Grazing Incidence X-Ray Diffraction

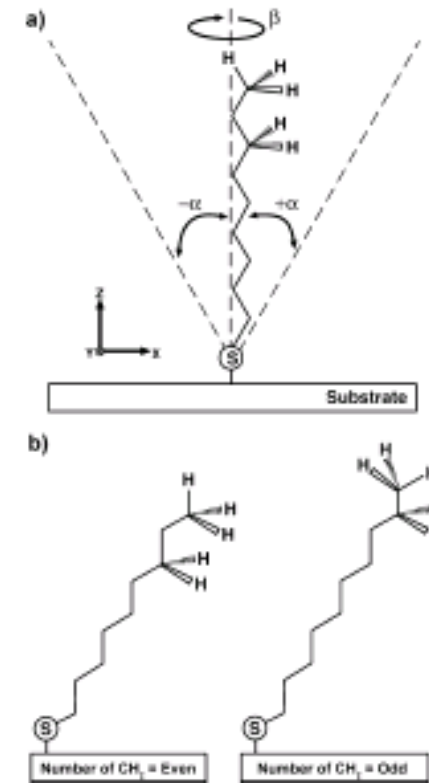
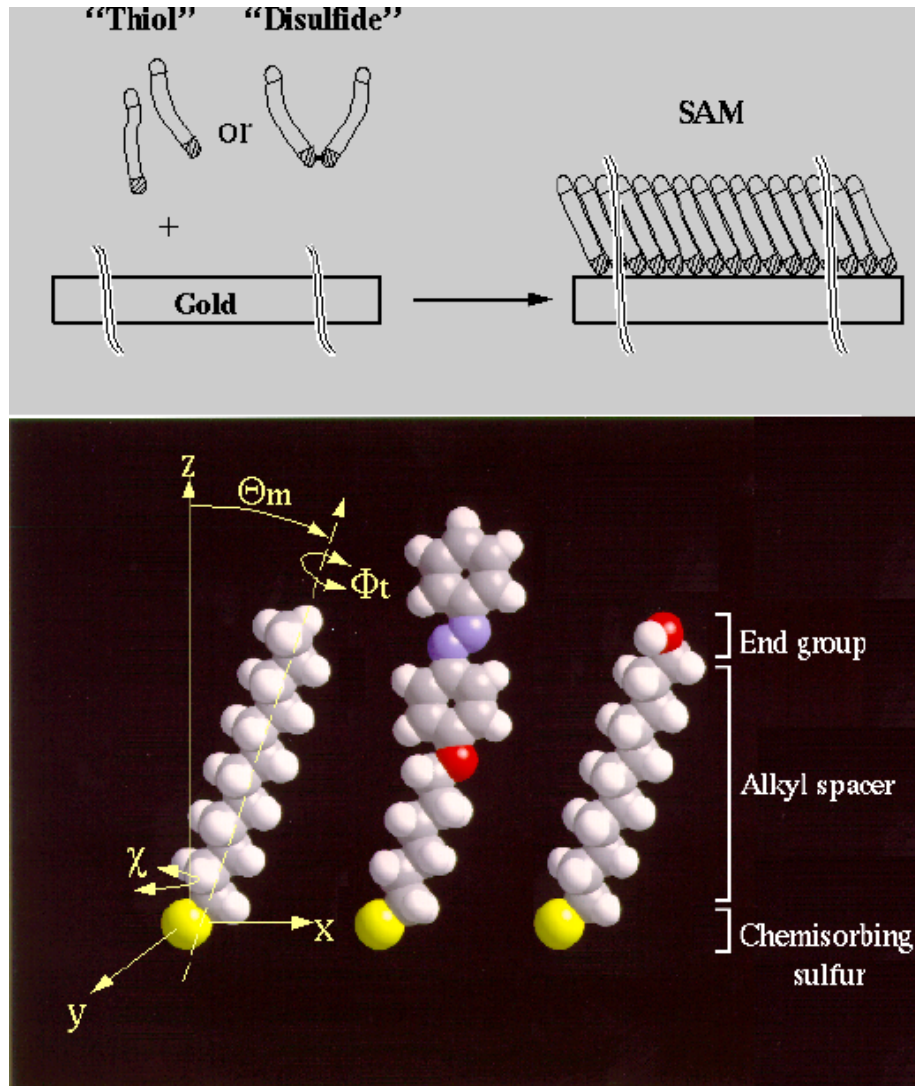


ALOISA beam line

Fig. 3. (A) Top view of the model resulting from GIXRD fit. Only the topmost Au layer with adatoms and S atoms of molecules are indicated. **(B)** Top view of the Au(111) surface with indications of the unit cells mentioned in the text. The conventionally termed $c(4 \times 2)$ corresponds to $c(2\sqrt{3} \times 4\sqrt{3})$, whose primitive cell is $(2\sqrt{3} \times 3)$, as depicted in the model. Note that as a result of the zigzag geometrical constraint (see text for explanation), the two S atoms in bridge sites [labeled m1 in (A)] are inequivalent because they bridge two different Au pairs, namely the atom pairs 3-2 and 3-5. The average S-Au bond length results are 2.42 Å and 2.37 Å for RS in bridge and RS-Au-SR geometry, respectively.



2D-SAMs



2D-SAMs

surface analysis and spectroscopic/physical characterization

RAIRS, reflectance absorption infrared spectroscopy

Raman spectroscopy

XPS: X-ray photoelectron spectroscopy

HREELS: high-resolution electron energy loss spectroscopy

NEXAFS: near edge X-ray absorption fine structure spectroscopy diffraction

helium atom scattering

X-ray diffraction

contact angle goniometry

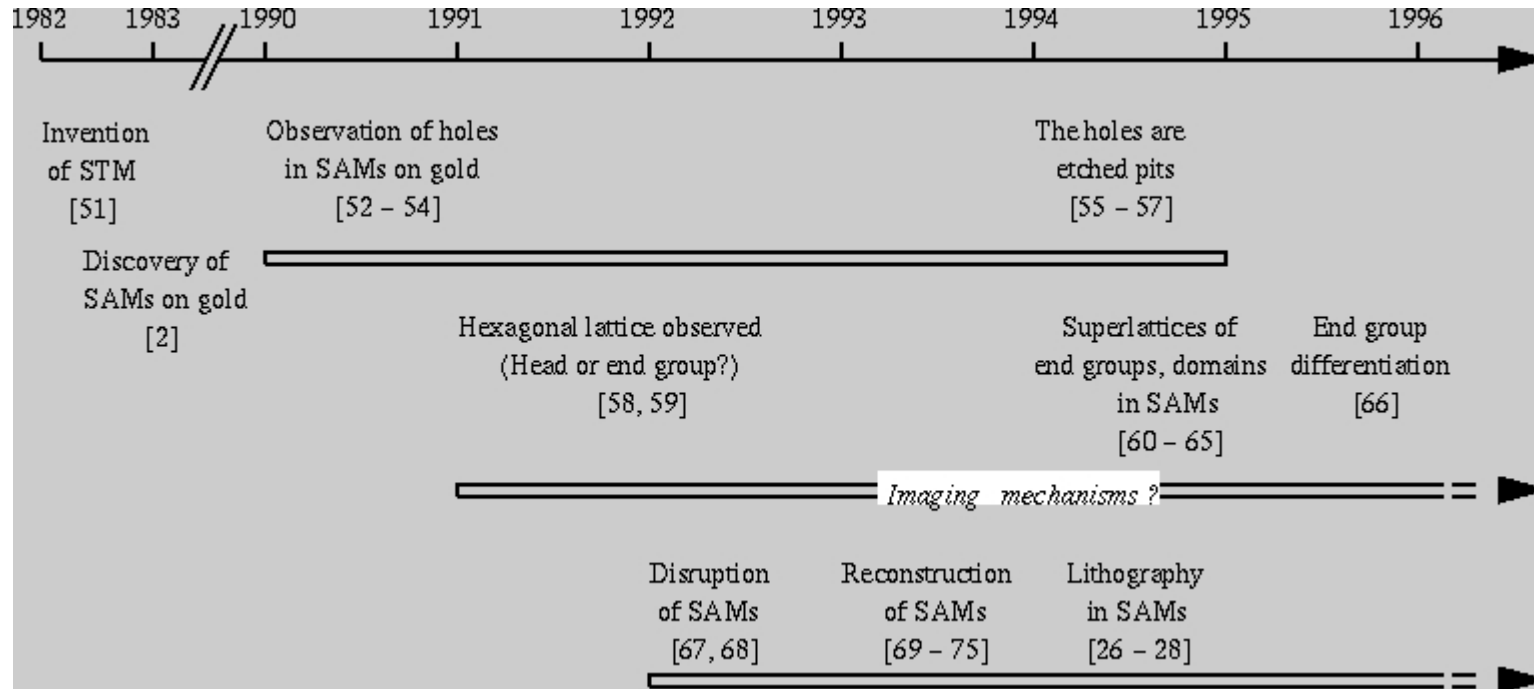
optical ellipsometry

SPR: surface plasmon resonance spectroscopy

mass spectrometry

SPM: scanning probe microscopy (AFM, STM)

2D-SAMs



STM

Scanning tunneling microscopy (STM) is a laboratory technique capable of obtaining atomic-scale resolution images of surfaces.

Gerd Binnig and **Heinrich Rohrer** at the IBM R schlikon laboratory have succeeded in creating an instrument with stable vacuum awarded in the 1986 Nobel Prize in physics

si basa sul principio di **quantum tunneling**

tip - conduttore

superficie metallica o di materiale semiconduttore

dalla superficie al tip ci pu  essere passaggio di elettroni

per effetto tunnel. A basi voltaggi la variazione di corrente  

una funzione della local density of states (LDOS)

del campione

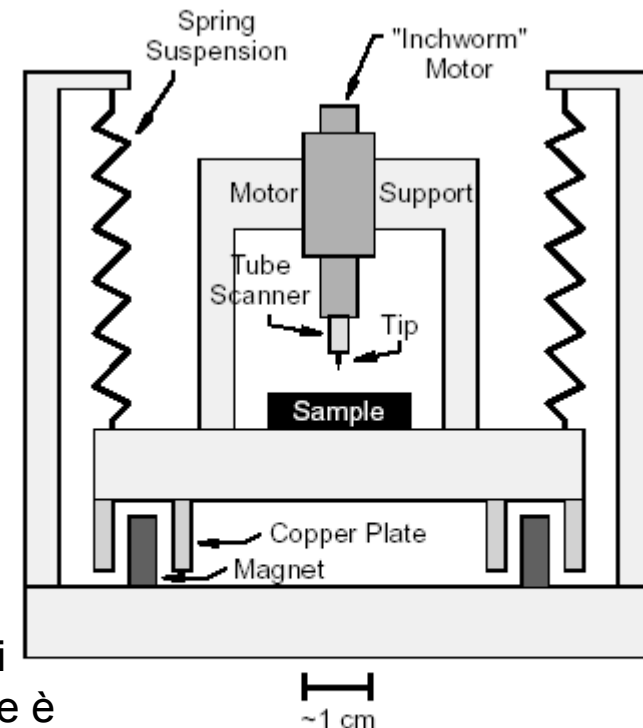
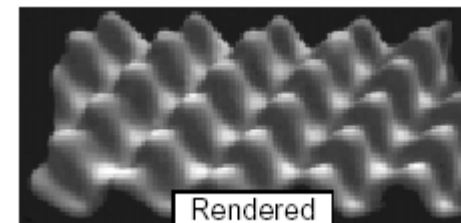
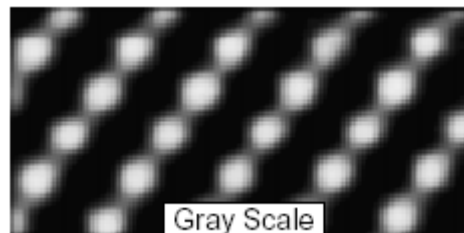
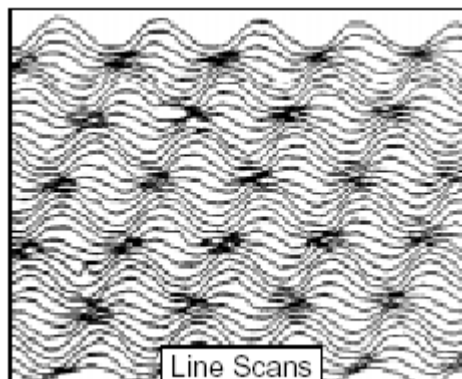
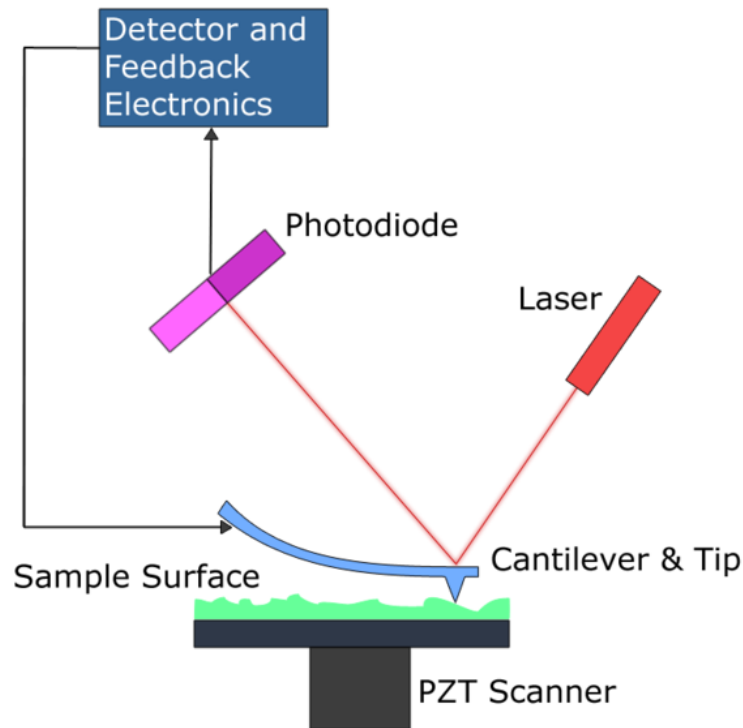


FIG. 3. Common elements of an STM, including a tip mounted on a piezoelectric tube scanner, a coarse approach mechanism (in this case an "inchworm" motor), and a damped vibration isolation system.

AFM

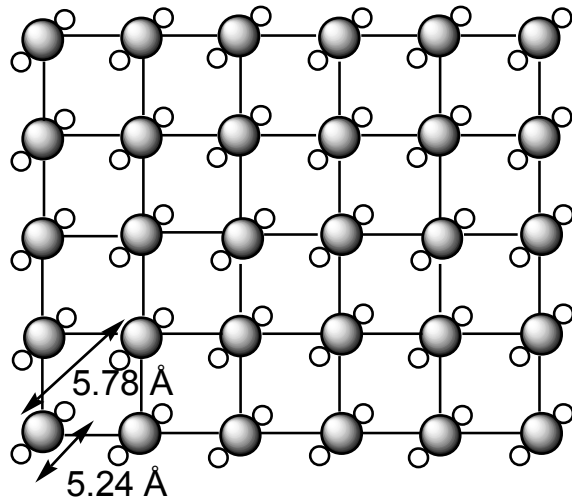
Atomic Force Microscopy, or Scanning Force Microscopy (SFM)



The AFM consists of a microscale cantilever with a sharp tip (probe) at its end that is used to scan the specimen surface. The cantilever is typically silicon or silicon nitride with a tip radius of curvature on the order of nanometers. When the tip is brought into proximity of a sample surface, forces between the tip and the sample lead to a deflection of the cantilever according to Hooke's law. Depending on the situation, forces that are measured in AFM include mechanical contact force, Van der Waals forces, capillary forces, chemical bonding, electrostatic forces, magnetic forces (see Magnetic force microscope (MFM)), Casimir forces, solvation forces etc.

2D-SAMs

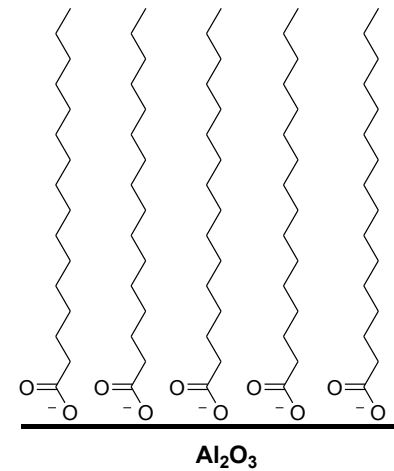
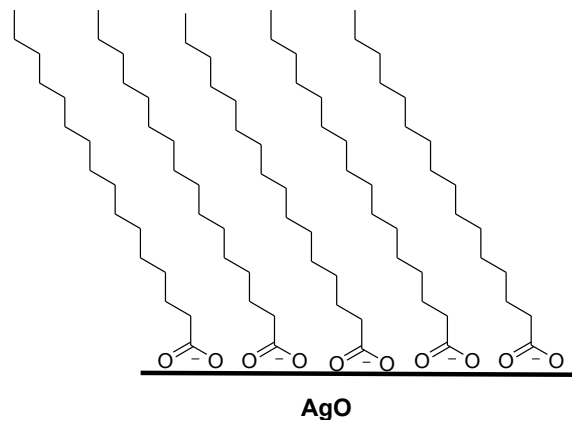
$C_nH_{2n+1}COOH$ on AgO



driving force: formation of a surface salt between the carboxylate anion and a surface metal cation, it is an acid-base reaction.

The p(2x2) adsorption scheme of fatty acids on AgO. The filled circles are the carboxylate carbon atoms, while the small, hollow circles are carboxylate oxygen atoms.

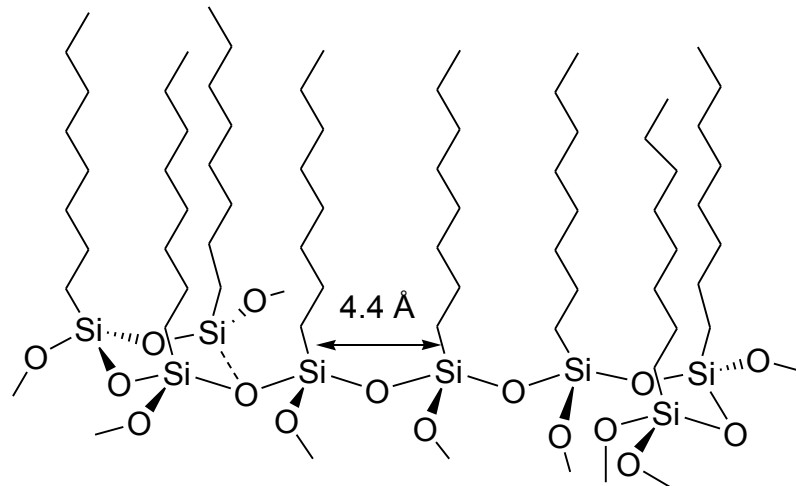
The alky chains are in all-trans extended configuration, and are tilted 26.7° from the surface normal.



2D-SAMs

alkylsilanes on: SiO_2 , Al_2O_3 , quartz, glass, mica,
ZnSe, GeO, Au

driving force: in situ formation of polysiloxane



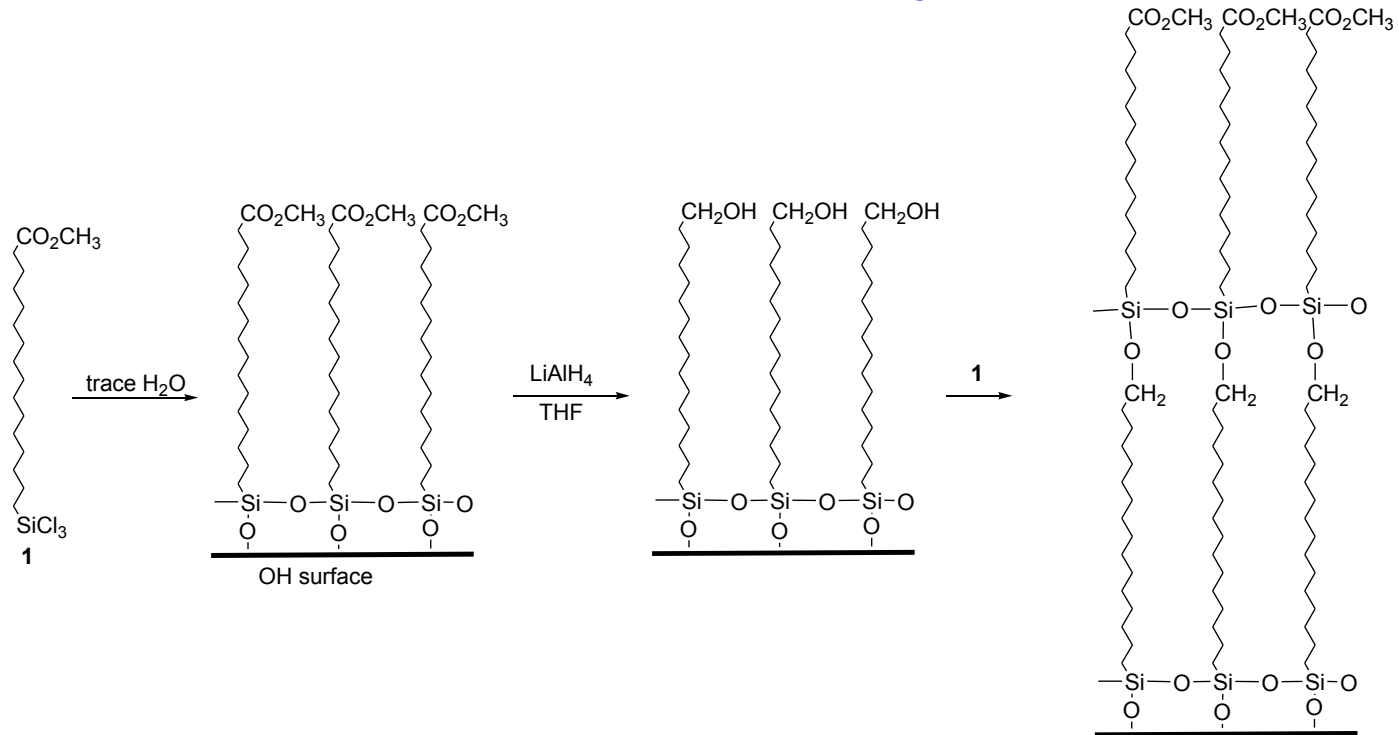
a tilt angle of about 10° from the normal has been observed

A schematic description of a polysiloxane at the monolayer-substrate surface.

The reproducibility of alkyltrichlorosilane monolayers is still a problem since the quality of the monolayer formed is very sensitive to reaction conditions.

2D-SAMs

modification of surface properties
construction of self-assembled multilayers

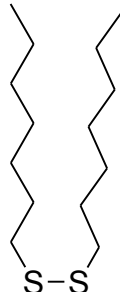


2D-SAMs

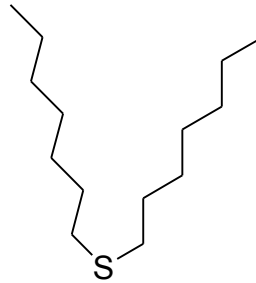
organosulfur adsorbates on gold



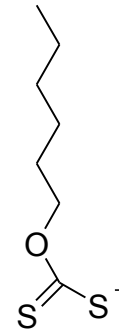
alkylthiol



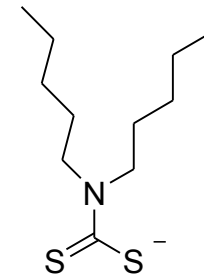
dialkyl disulfide



dialkyl sulfide



alkyl xanthate



dialkylthiocarbamate

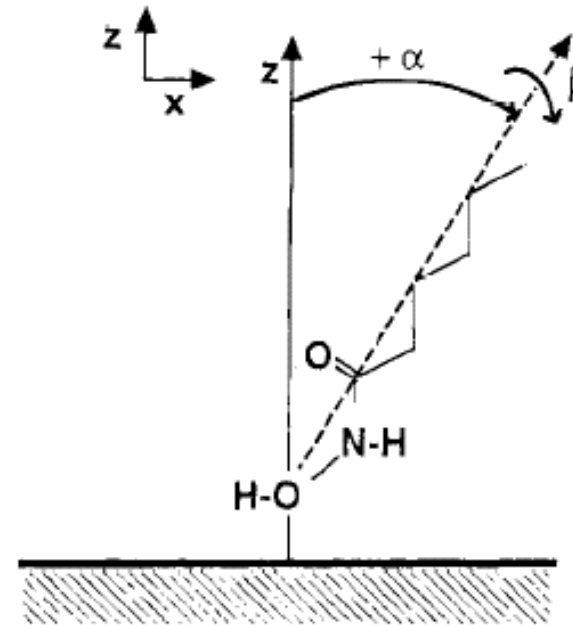
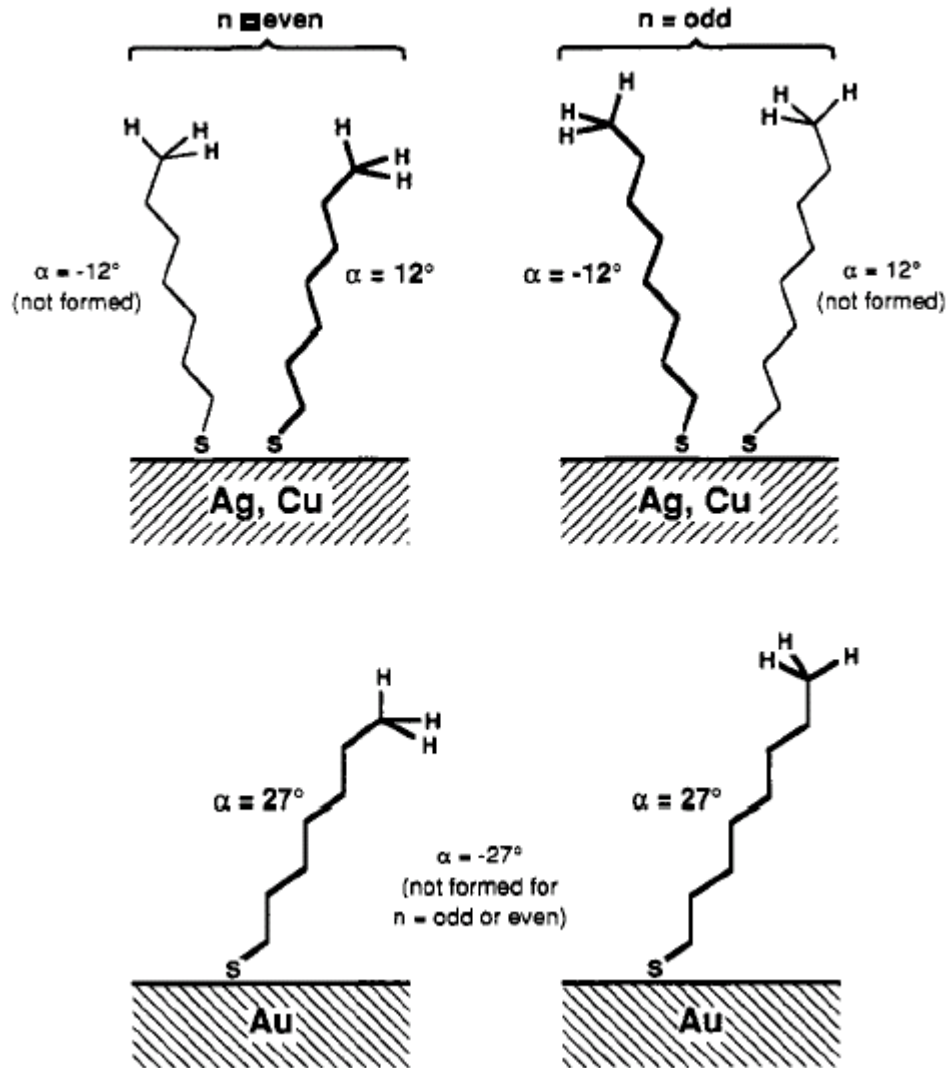
also on: Ag, Cu, Pt, Hg, Fe,
nanoparticles as: γ -Fe₂O₃, GaAs, InP

bond	bond energy, Kcal/mol, (KJ/mol)
------	------------------------------------

S-H	87,26 (363)
-----	-------------

S-S	54,32 (226)
-----	-------------

2D-SAMs



MOx	α	β
Cu	$ 20^\circ $	54°
Ag	-14°	38°
Al	$ 8^\circ $	47°
Ti	---	---

(RSH on Pd: $|\alpha| \approx 10^\circ$)

Folkers, John P.; et al. *Langmuir* **1995**, *11*, 813.

Laibinis, Paul E.; Whitesides, G. M.; et al. *J. Am. Chem. Soc.* **1991**, *113*, 152.

2D-SAMs

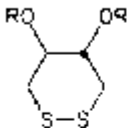
Adsorption of Bifunctional Organic Disulfides on Gold Surfaces

Ralph G. Nuzzo* and David L. Allara*

Bell Laboratories, Murray Hill, New Jersey 07974

Received January 20, 1983

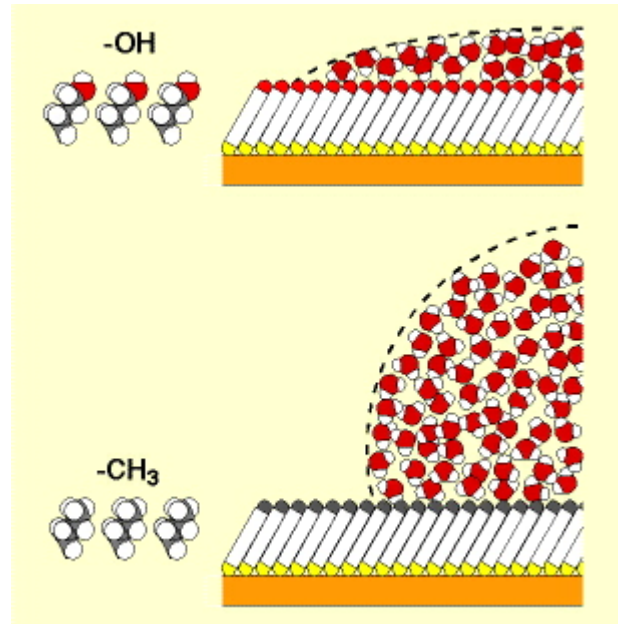
Table I. Solution Adsorption of Organic Disulfides on Evaporated Gold Films at Room Temperature

 <i>d,t</i> R -	thickness of film by ellipsometry, ^{a-c} Å	estimated max vert. extension of adsorbed molecules with attachment at the S-S group, ^f Å	contact angle of water, deg ^g
CF ₃ (CF ₂) ₆ CO (1a)	10.5 ± 1.0 ^d	15.5, 11 ^e	104 ± 1
CH ₃ (CH ₂) ₁₄ CO (1b)	20.5 ± 1.0 ^e	25	96 ± 1
O ₂ NC ₂ H ₄ CO (1c)	9.5 ± 2.5	12.5	52 ± 2
CH ₃ CO (1d)	7.0 ± 2.5	8	47 ± 1
CF ₃ CO (1e)	4.0 ± 0.5	9	57 ± 1
H (1f)	5.0 ± 0.5	6	34 ± 1
(HO ₂ C(CH ₂) ₂ S) ₂ (2)	4.0 ± 0.5	6 ^h	13 ± 2
(CH ₃ (CH ₂) ₁₁ S) ₂ (3)	21.5 ± 1.0	22 ^h	99 ± 1

J. Am. Chem. Soc. **1983**, *105*, 4481-4482.

2D-SAMs

wetting behaviour



BAGNABILITA'

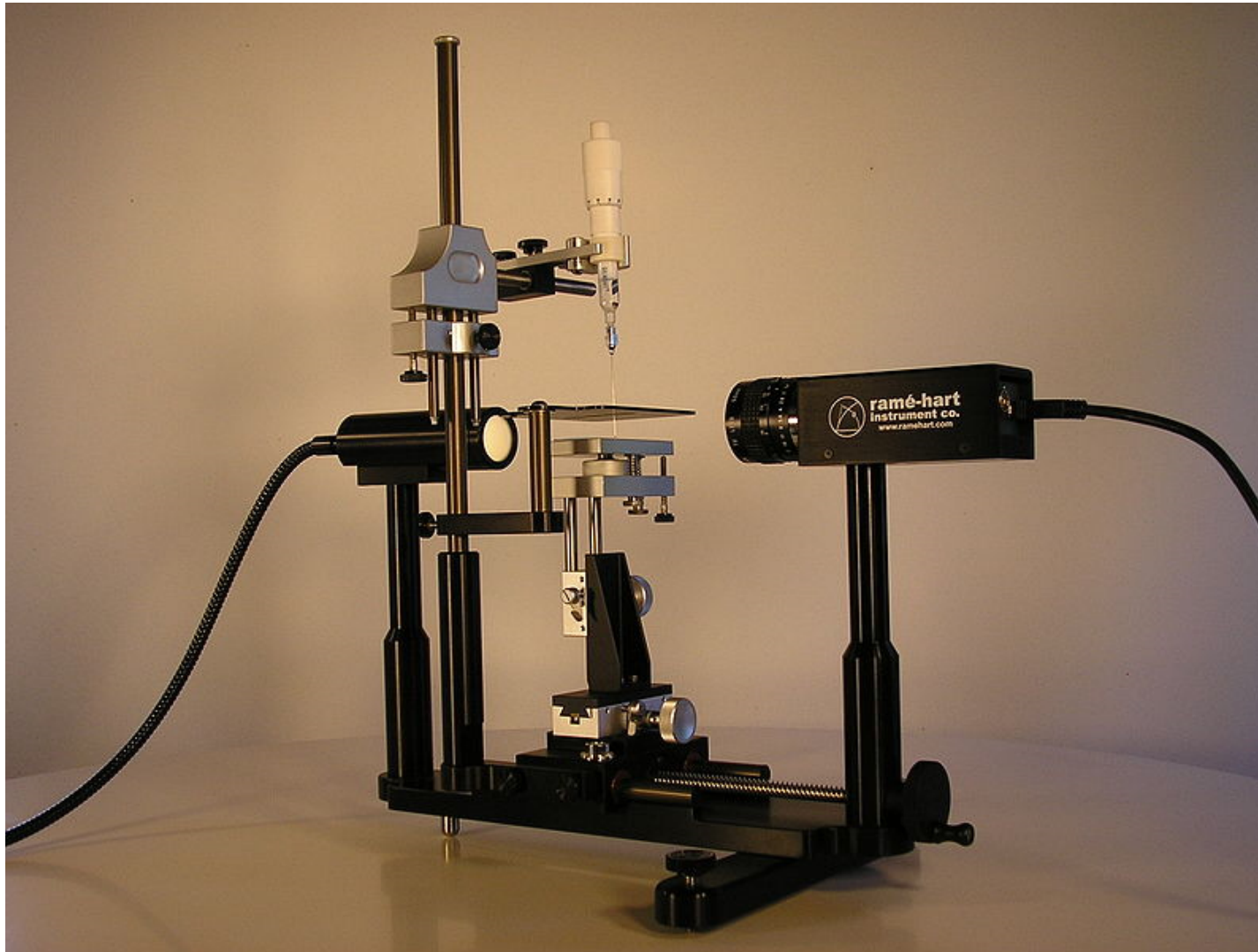
Perchè un tessuto asciuga bene l'acqua mentre un altro sembra rifiutarla? Perchè l'acqua si raccoglie in grosse gocce su di una superficie unta e forma invece un film aderente su di una superficie pulita? Una goccia di un liquido che venga deposta su di una superficie solida vi aderisce in modo maggiore o minore a seconda della natura del liquido e di quella del solido. Per comprendere questo fenomeno bisogna considerare che le molecole di un liquido sono soggette ad una **forza di coesione** che le mantiene unite le une alle altre, ma esiste anche una **forza di adesione** che rappresenta la forza con cui le molecole del liquido aderiscono alla superficie di un materiale con cui vengono in contatto. Quando le forze di adesione sono grandi rispetto alle forze di coesione, il liquido tende a bagnare la superficie, quando invece le forze di adesione sono piccole rispetto a quelle di coesione, il liquido tende a "rifiutare" la superficie. A questo proposito si parla di bagnabilità fra liquidi e solidi. Per esempio, l'acqua bagna il vetro pulito, ma non bagna la cera.

1 - **Misura dell'angolo di contatto.** Deponete una goccia di un liquido su di una superficie liscia di un solido. A seconda della bagnabilità del liquido nei confronti di quel solido, la goccia formerà un determinato angolo di contatto con il solido. In riferimento alla figura 10, se l'angolo di contatto è inferiore a 90° , il solido viene definito bagnabile, se l'angolo di contatto è maggiore di 90° , il solido viene definito non bagnabile. Un angolo di contatto pari a zero indica completa bagnabilità. Per misurare l'angolo di contatto usate un goniometro ed un righello. Fare una fotografia



Figura 10 - L'angolo di contatto di un liquido con un solido viene utilizzato come indice di bagnabilità. Per $\alpha < 90^\circ$ il liquido bagna la parete (es: acqua su vetro), per $\alpha > 90^\circ$ il liquido non bagna la parete (es: mercurio su vetro). Se $\alpha = 0^\circ$ si dice che il liquido bagna perfettamente la parete.

misura dell' angolo di contatto

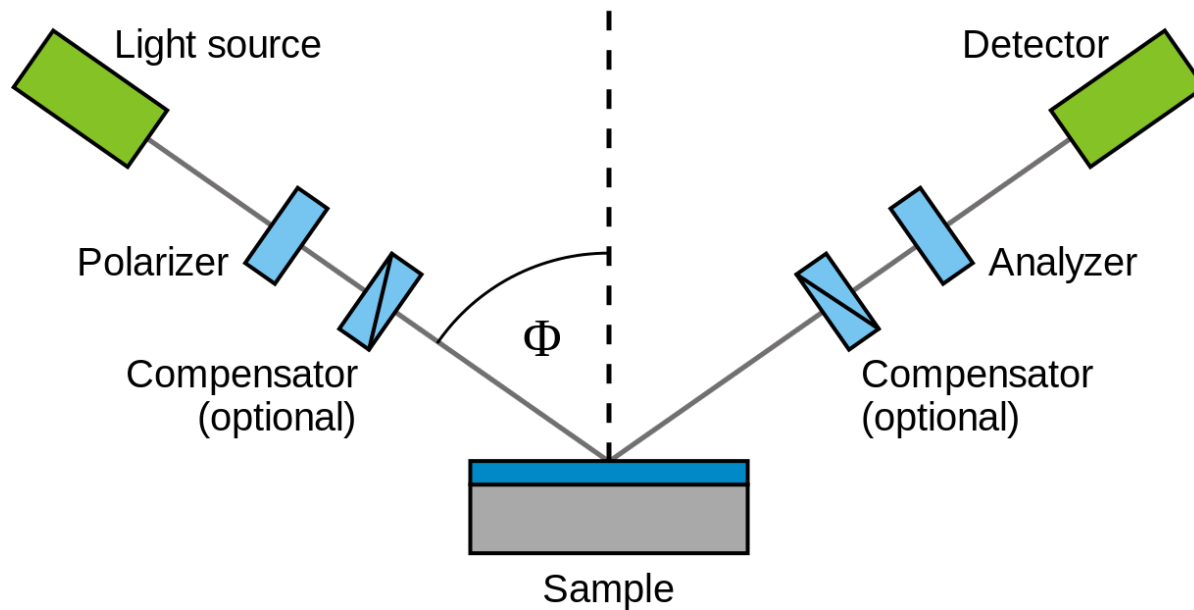


Surface scientists use a contact angle goniometer to measure contact angle, surface energy and surface tension.

ELLIPSOMETRY

Ellipsometry is an optical technique for investigating the dielectric properties (complex refractive index or dielectric function) of thin films.

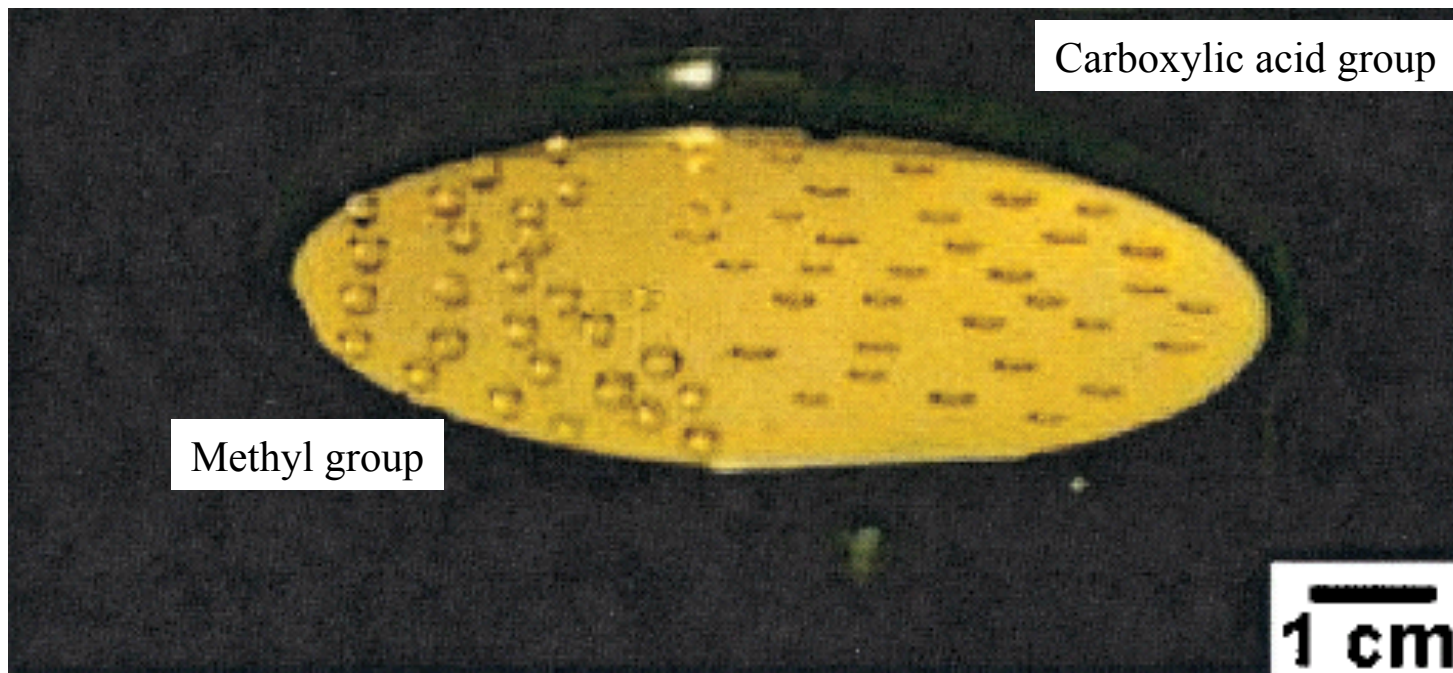
Ellipsometry can be used to characterize composition, roughness, thickness (depth), crystalline nature, doping concentration, electrical conductivity and other material properties. It is very sensitive to the change in the optical response of incident radiation that interacts with the material being investigated.



Ellipsometry measures the change of polarization upon reflection or transmission and compares it to a model. The exact nature of the polarization change is determined by the sample's properties (thickness, complex refractive index or dielectric function tensor)

Changing Functional Groups

Surface Polarity



Surface-Chemical Gradients

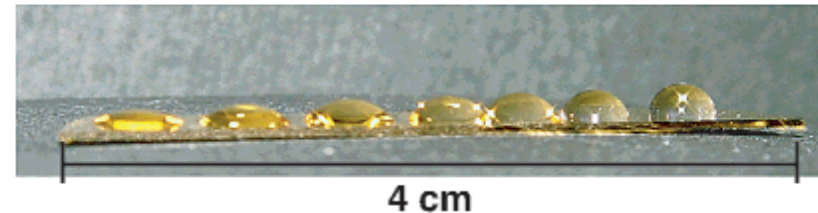
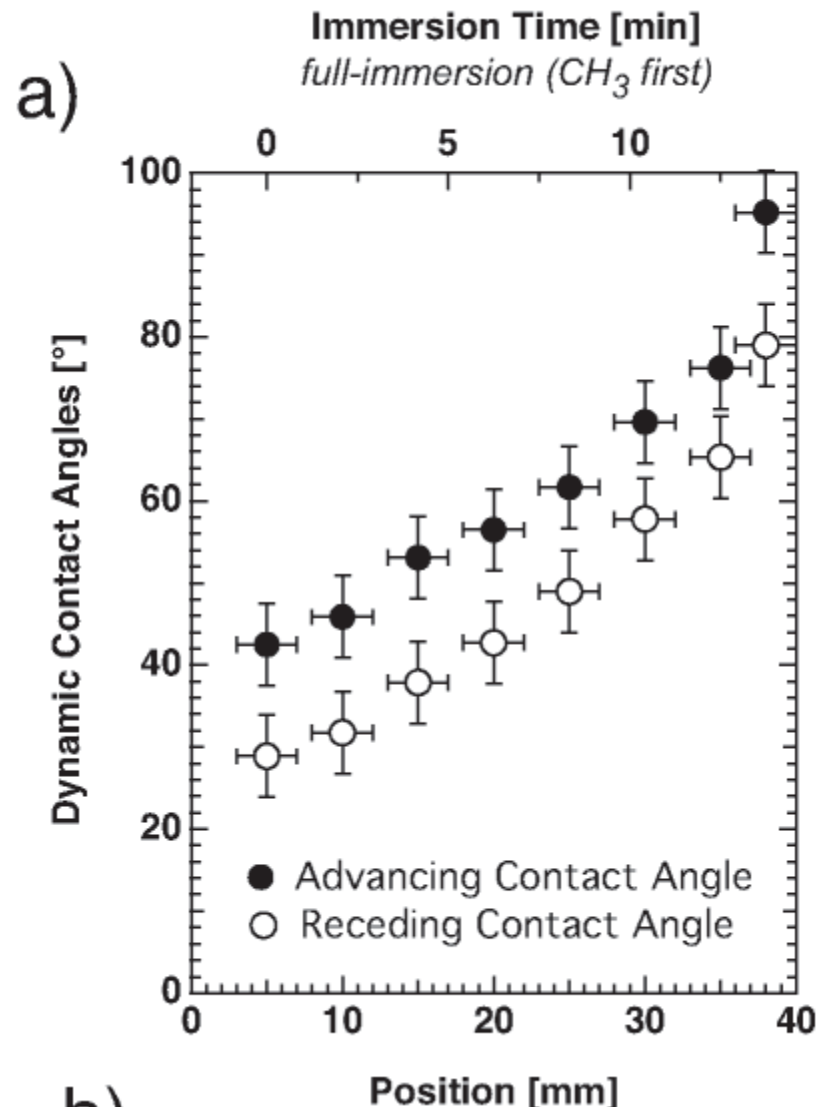
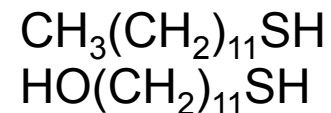
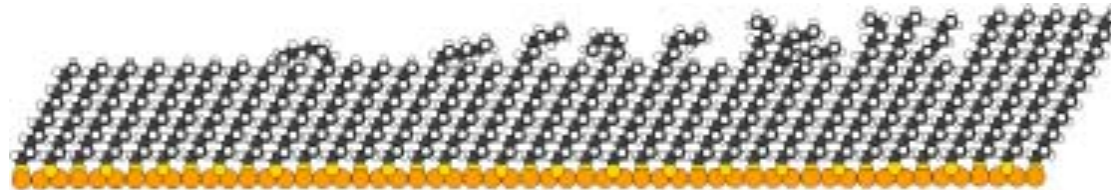
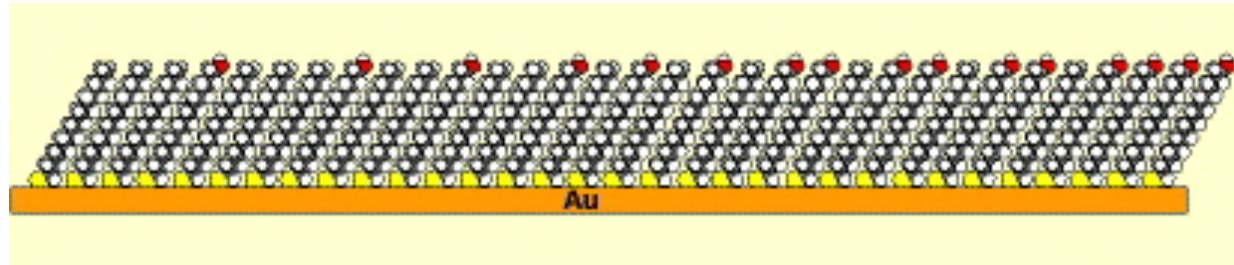


Figure 2. (a) Dynamic contact angles along a hydrophobicity gradient using *full-immersion (CH₃-first)* as the preparation method. The small hysteresis of less than 15° between the advancing and the receding contact angles is an indication for the formation of a full monolayer. (b) Water droplets along a hydrophobicity gradient using *full-immersion (CH₃-first)* as the preparation method.



2D-SAMs



surfaces with different functional groups have been reported, for example:
 CF_3 , $\text{CH}=\text{CH}_2$, $\text{C}\equiv\text{CH}$, Cl , Br , CN , OH , OCH_3 , NH_2 , $\text{N}(\text{CH}_3)_2$, SO_3H ,
 $\text{Si}(\text{OCH}_3)_3$, COOH , COOCH_3 , CONH_2 , etc.

2D-SAMs

Langmuir 1998, 14, 6693–6698

Flat Lying Pin-Stripe Phase of Decanethiol Self-Assembled Monolayers on Au(111)

R. Staub, M. Toerker, T. Fritz, T. Schmitz-Hübsch, F. Sellam, and K. Leo*

decanethiol self-assembled monolayers on Au(111)

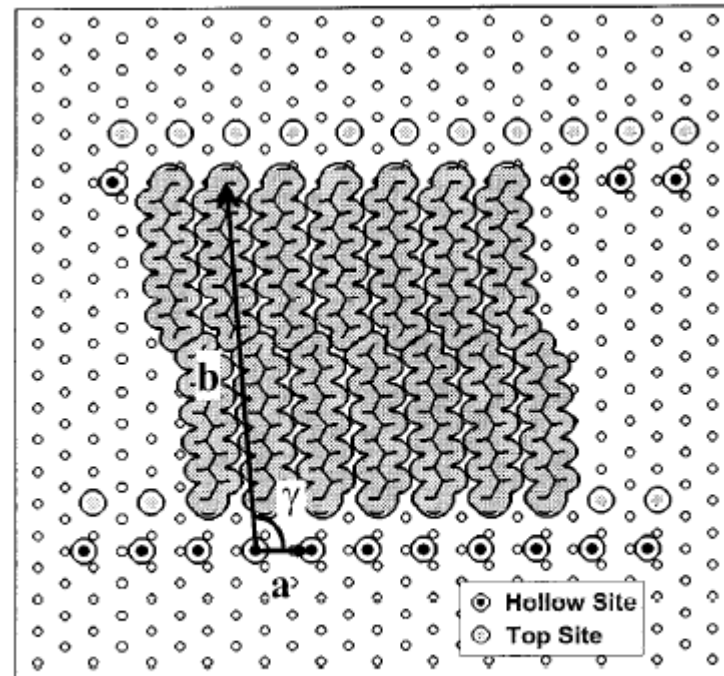
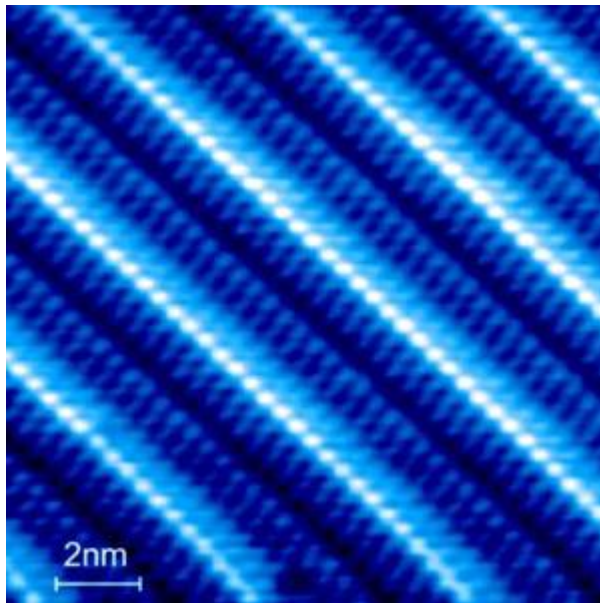


Figure 6. Real space structure model for the $11.5 \times \sqrt{3}$ pin-stripe structure of decanethiol.

2D-SAMs

defects on SAMs

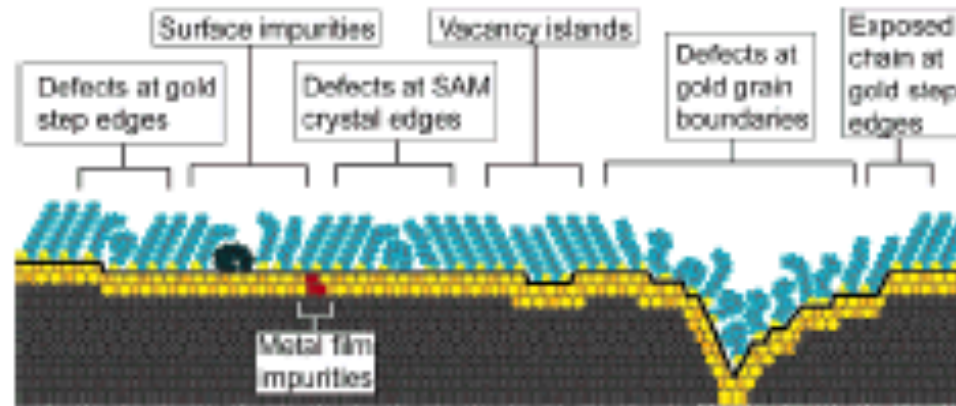
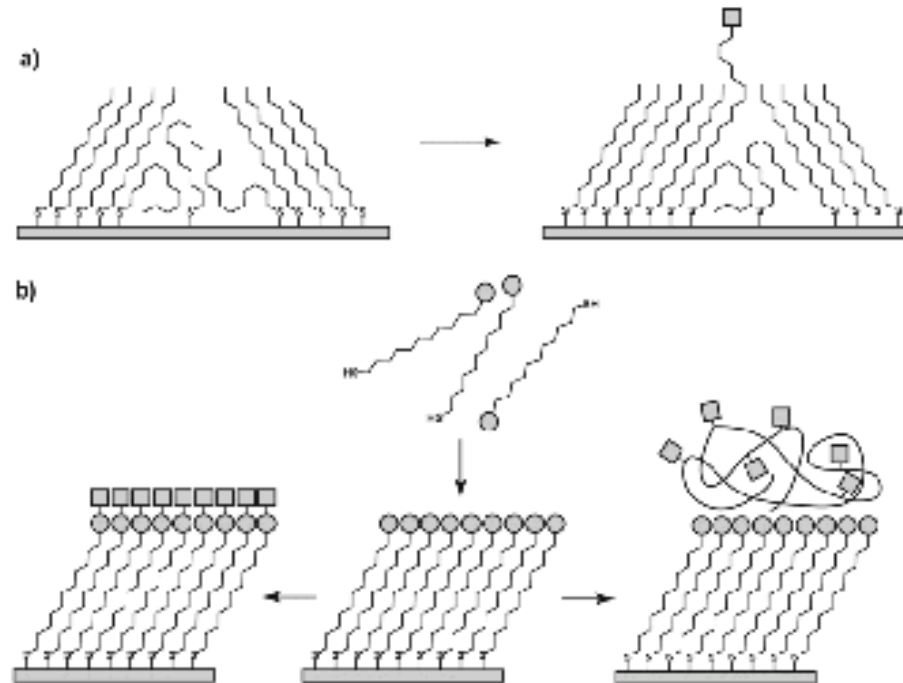


Figure 7. Schematic illustration of some of the intrinsic and extrinsic defects found in SAMs formed on polycrystalline substrates. The dark line at the metal-sulfur interface is a visual guide for the reader and indicates the changing topography of the substrate itself.

2D-SAMs

surface modifications

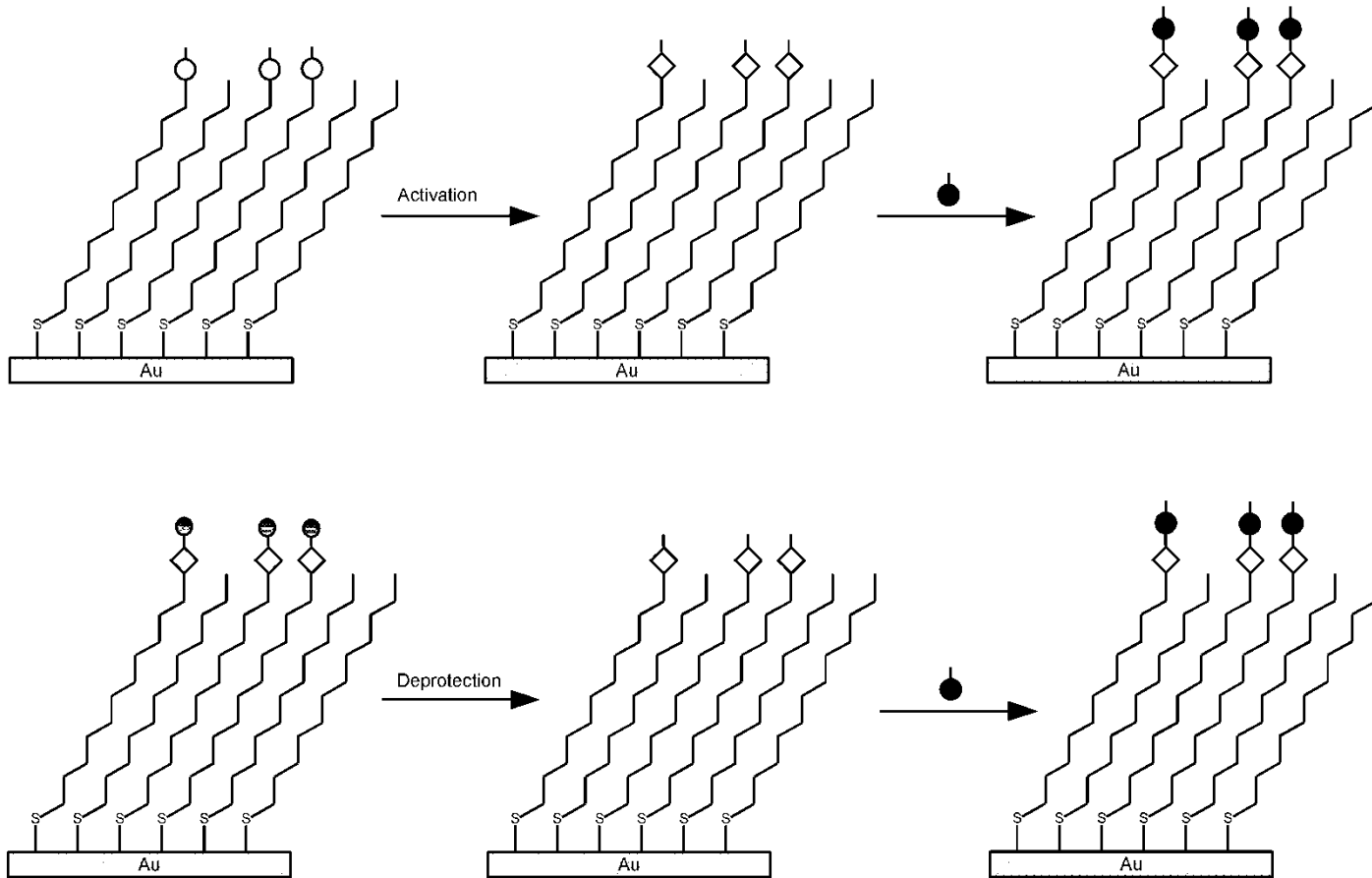
Scheme 1. General Strategies for Modifying the Interfacial Composition of SAMs after Formation^a



^a (a) Insertion of a functional adsorbate at a defect site in a preformed SAM. (b) Transformation of a SAM with exposed functional groups (circles) by either chemical reaction or adsorption of another material.

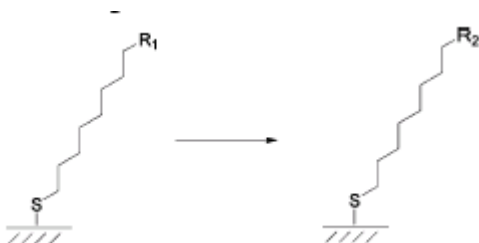
2D-SAMs

surface modifications



2D-SAMs

surface modifications



surface group R ₁	reagent	product

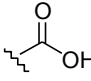
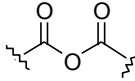
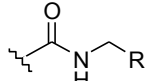
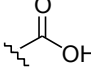
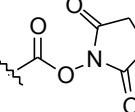
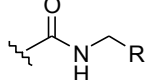
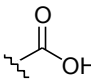
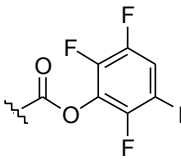
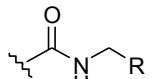
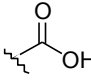
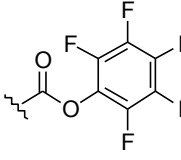
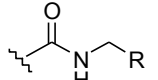
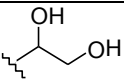
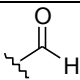
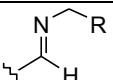
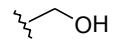
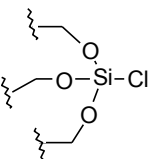
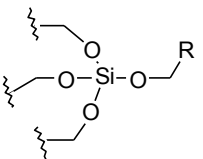
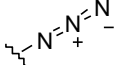
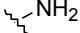
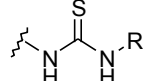
Table 4.2 Selected Methods for SAMs Functionalization via the Formation of Activated Species

Surface bound reactive group	Activated species	Reagent	Product	Reference
		$R-NH_2$		57
		$R-NH_2$		72
		$R-NH_2$		59
		$R-NH_2$		58
		$R-NH_2$		61-63
		$R-OH$		64
		$R-N=C=S$		71, 78

2D-SAMs

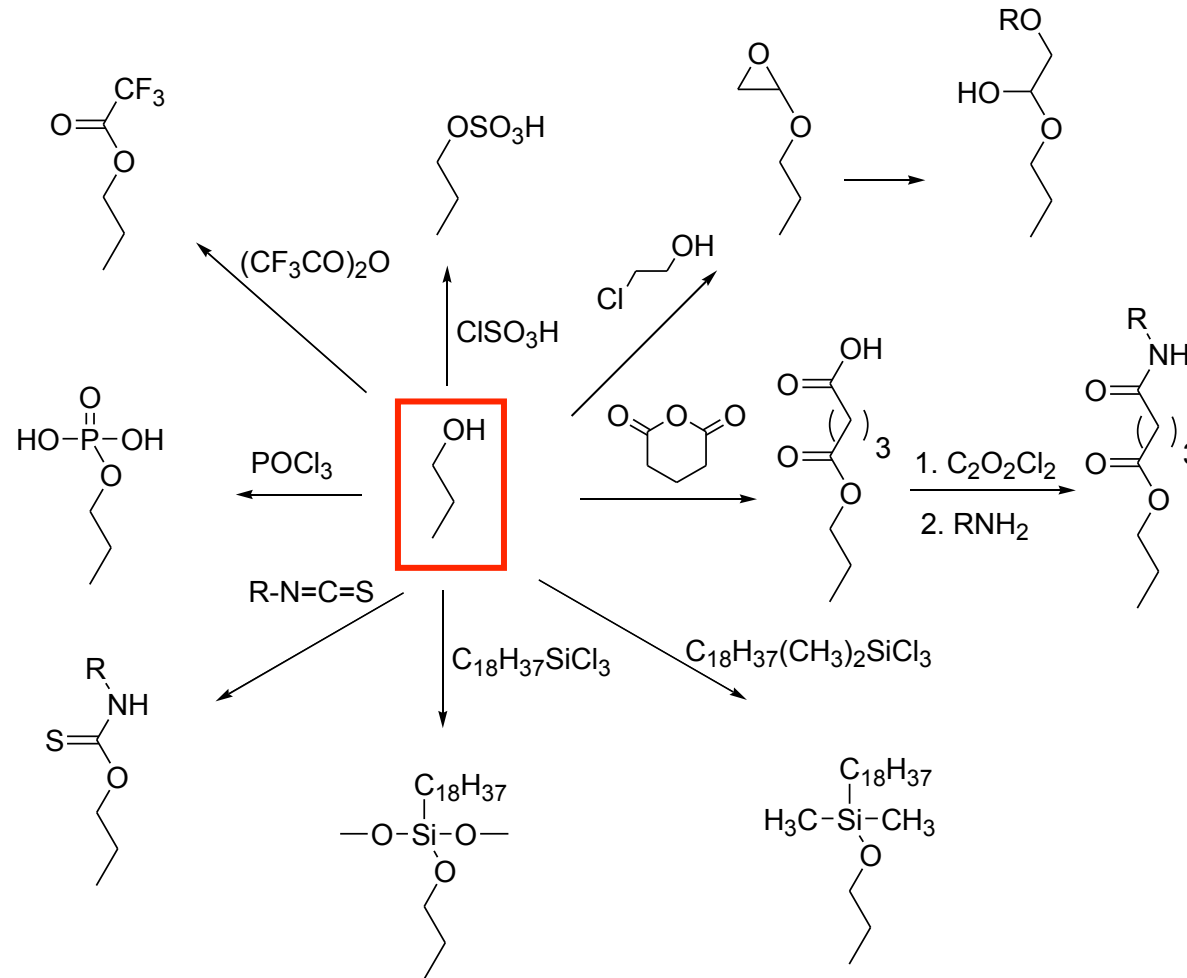
surface modifications

Selected methods for SAMs functionalization via the formation of activated species.

Surface Bound Reactive Group	Activated Species	Reagent	Product
		$R-NH_2$	
		$R-NH_2$	
		$R-NH_2$	
		$R-NH_2$	
		$R-NH_2$	
		$R-OH$	
		$R-N=C=S$	

2D-SAMs

surface modifications



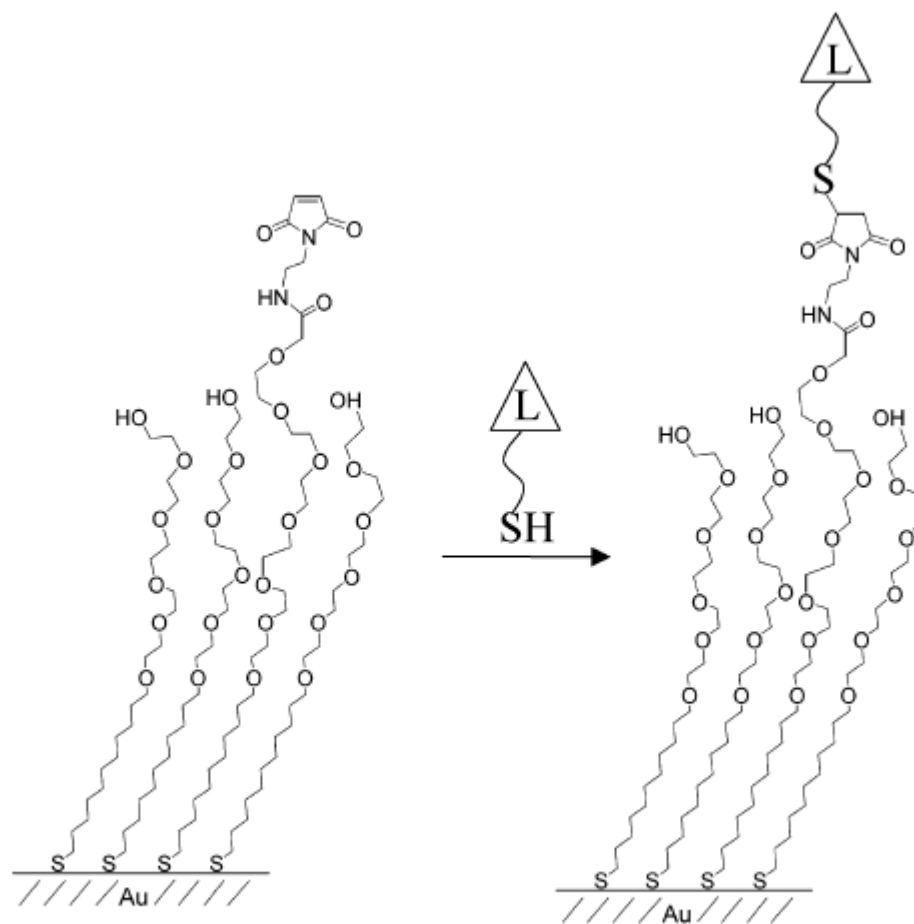
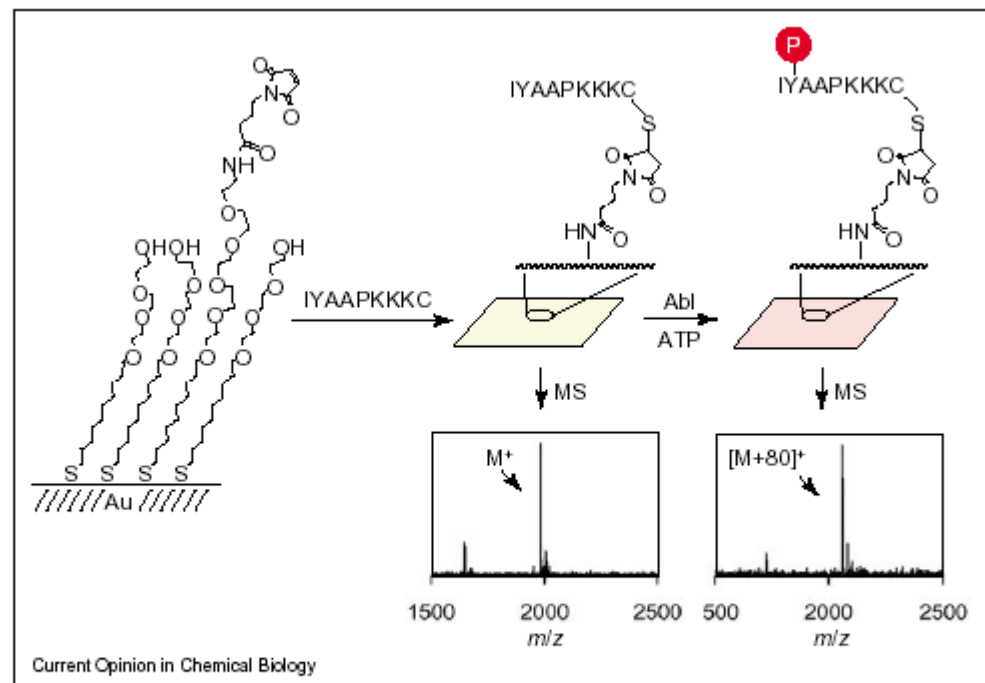


Figure 1. Structure of a self-assembled monolayer used to immobilized thiol-terminated ligands. The maleimide groups react selectively with thiol groups in a contacting solution while the penta(ethylene glycol) groups prevent the nonspecific adsorption of protein to the monolayer.

B. T. Houseman, E. S. Gawalt, M. Mrksich *Langmuir* **2003**, *19*, 1522-1531



Design of peptide arrays for characterizing enzyme activities by MALDI-TOF MS. A peptide substrate for Abl kinase was immobilized to a maleimide-presented self-assembled monolayer (SAM). The monolayer was treated with Abl kinase and phosphorylation was characterized by MALDI-TOF MS.

Label-Free Detection of Protein–Protein Interactions on Biochips**

Woon-Seok Yeo, Dal-Hee Min, Robert W. Hsieh,
Geoffrey L. Greene, and Milan Mrksich*

ACIE 2005, 44, 5480.

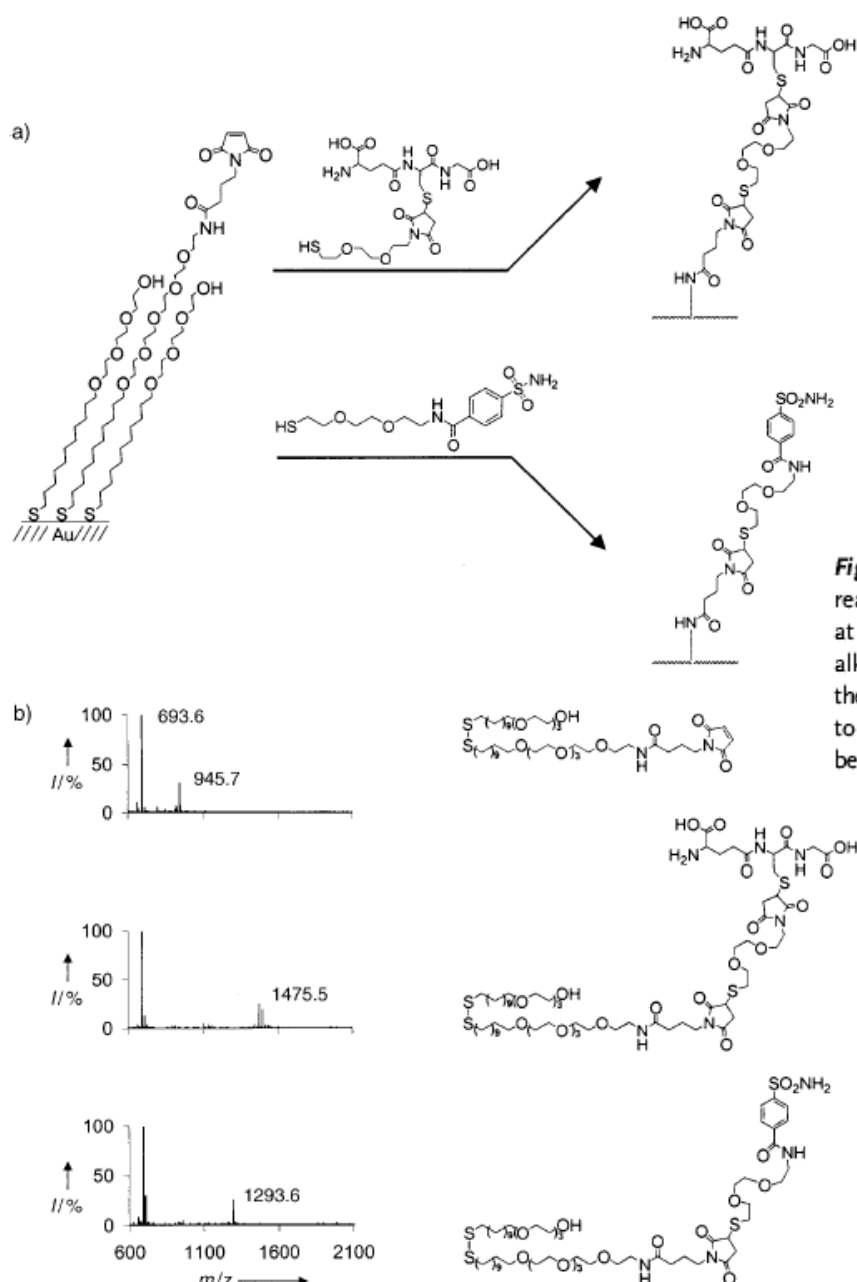


Figure 1. a) Protein-capture ligands were immobilized onto a maleimide-terminated SAM by reaction of the thiol-tagged ligands. b) MS data for the initial monolayer (top) displayed a peak at m/z 945.7, which corresponds to the mixed disulfide derived from a maleimide-terminated alkanethiolate and a tri(ethylene glycol)-terminated alkanethiolate. After treatment with ligands, the original peak disappeared and gave rise to a new peak at m/z 1475.5, which corresponds to the glutathione-conjugated product (middle) or at m/z 1293.6, which corresponds to the benzene sulfonamide-conjugated product (bottom).

Biomolecular Surfaces that Release Ligands under Electrochemical Control

J. Am. Chem. Soc. **2000**, *122*, 4235–4236

Christian D. Hodneland and Milan Mrksich*

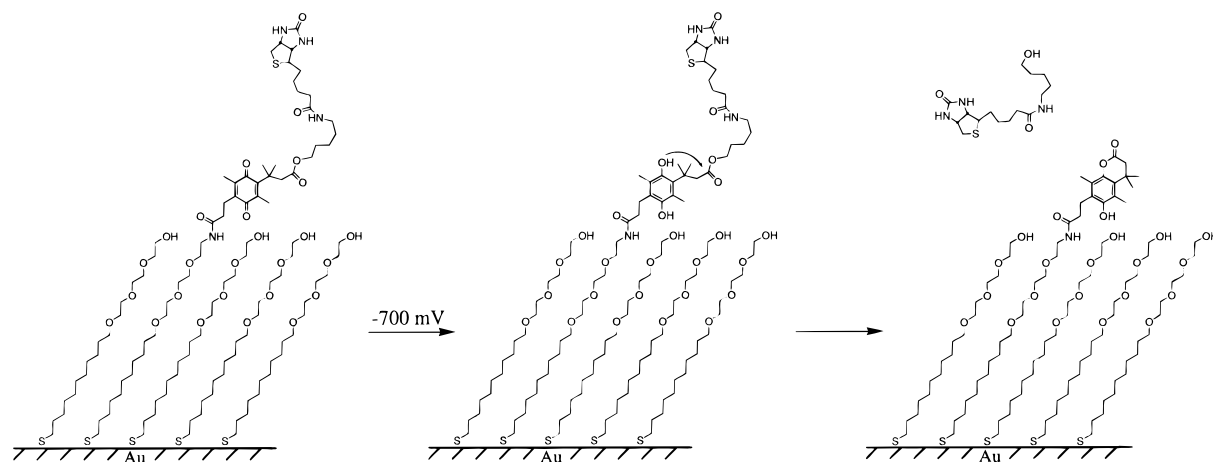


Figure 1. Design of a self-assembled monolayer (SAM) that selectively releases the ligand biotin upon application of a reductive potential. The ligand is tethered to the alkanethiolate through a quinone propionic ester and is present at a density of 1%. On application of a potential of -700 mV to the underlying gold film, the quinone is reduced to the hydroquinone, which then undergoes rapid lactonization with release of biotin. The tri(ethylene glycol) groups in the monolayer prevent the non-specific adsorption of protein.

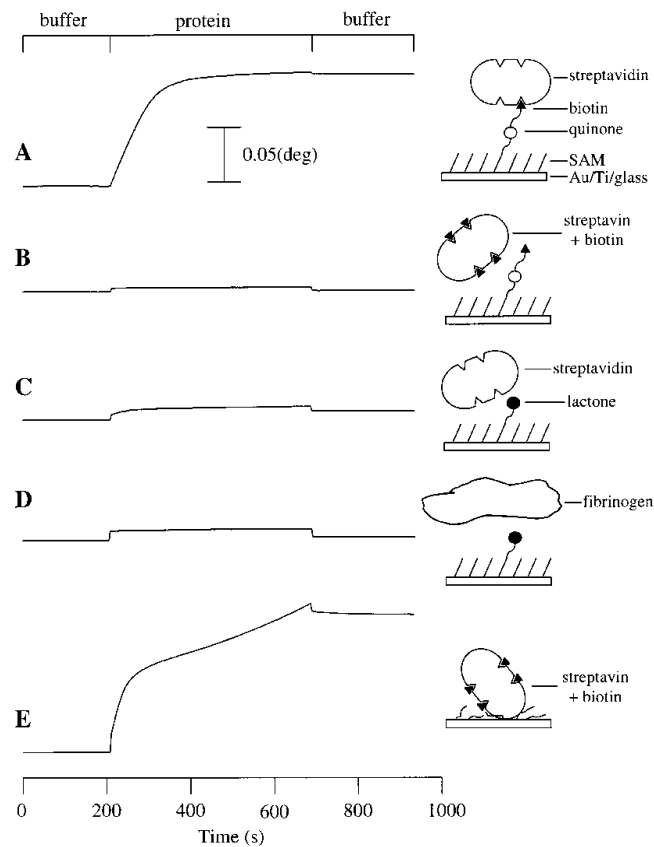
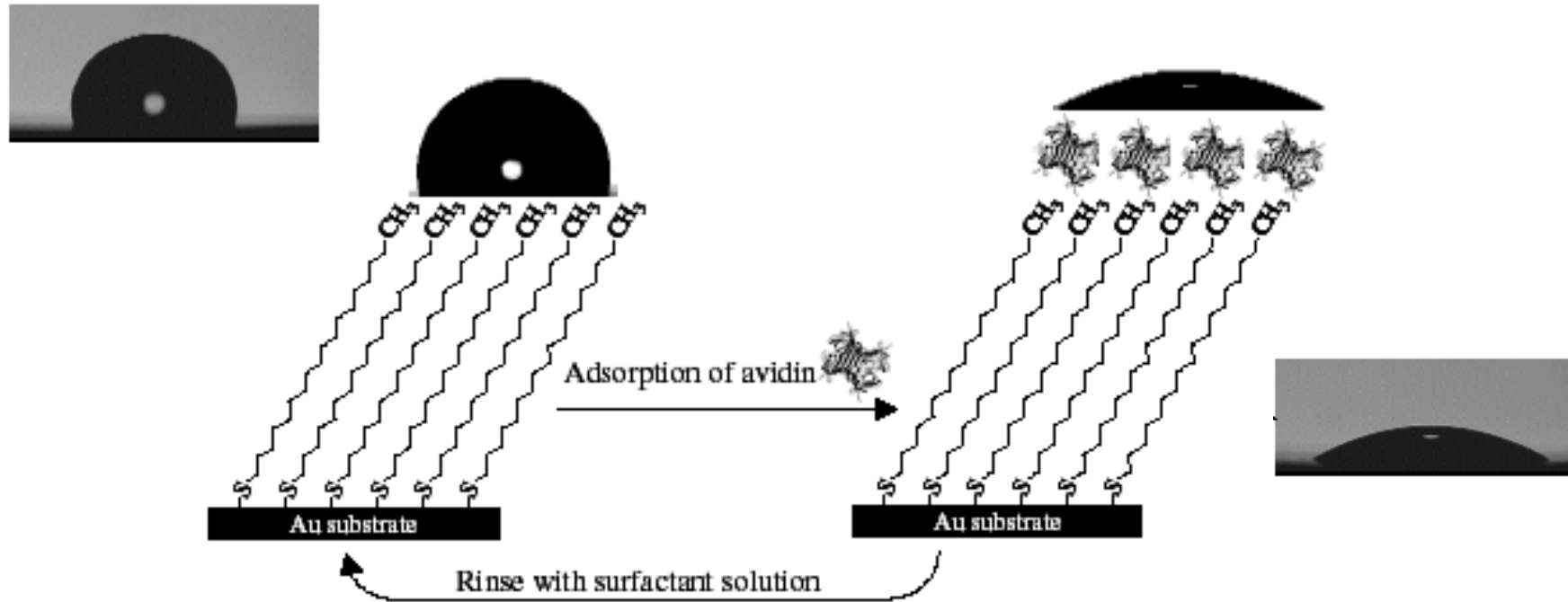


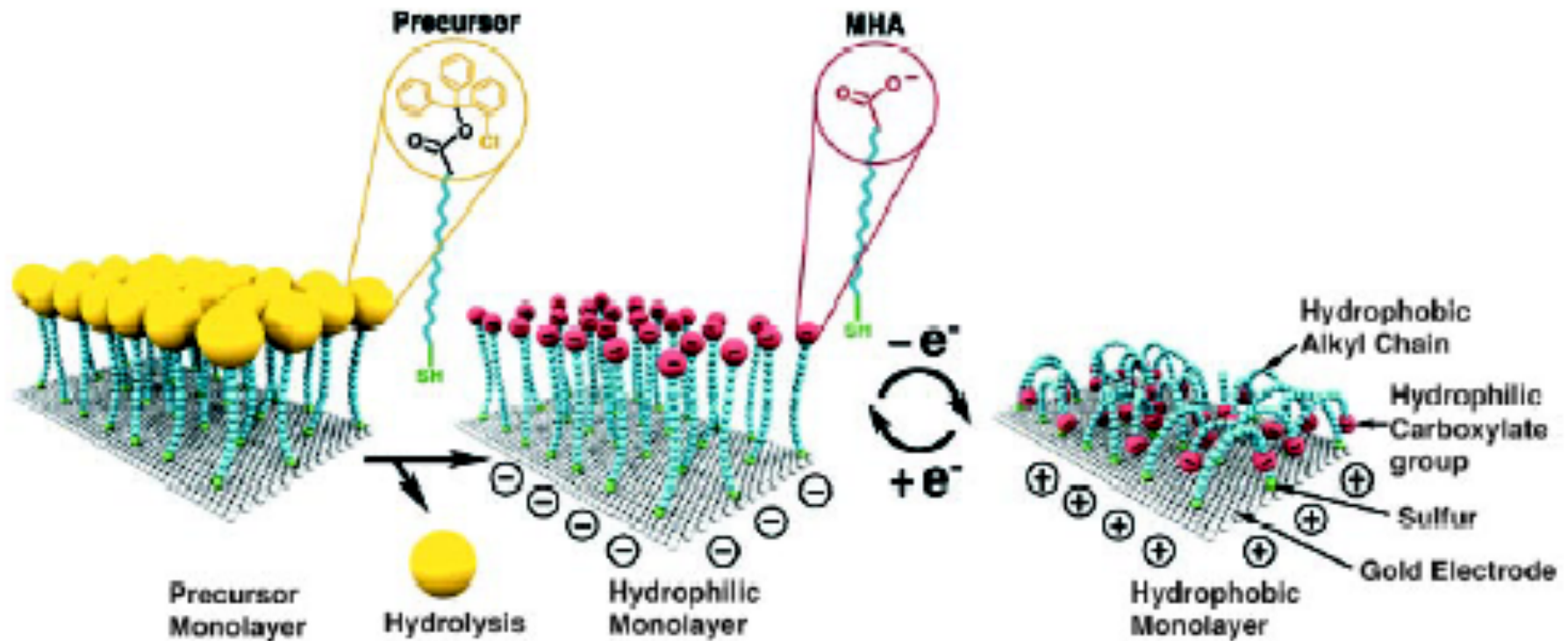
Figure 2. SPR data showing the association of proteins with the SAMs (see text for an explanation of the data). The change in resonance angle ($\Delta\theta$) is plotted on the vertical axis: the scale bar applies to all data, which are offset for clarity. (A) Streptavidin (60 nM) associated with a surface presenting biotin. (B) Streptavidin pre-incubated with biotin (140 μM) showed no association with the surface, demonstrating that the interaction is biospecific. (C) Application of a potential of -700 mV for 3 min to the monolayer, prior to the binding experiment, resulted in the release of ligand and a 95% reduction in streptavidin binding. (D) Fibrinogen (0.5 mg/mL) did not adsorb to the SAM following electrochemical treatment, demonstrating that the SAM remained inert to protein adsorption. (E) Application of a potential of -1100 mV for 5 min caused association of streptavidin pre-saturated with biotin, showing the surface was damaged and was no longer resistant to non-specific protein adsorption.

Reversible Hydrophobic/Hydrophilic Surfaces



Deval, J., et al., *J. Micromech. Microeng.* **2004**, *14*, 91.

Reversible Hydrophobic/Hydrophilic Surfaces

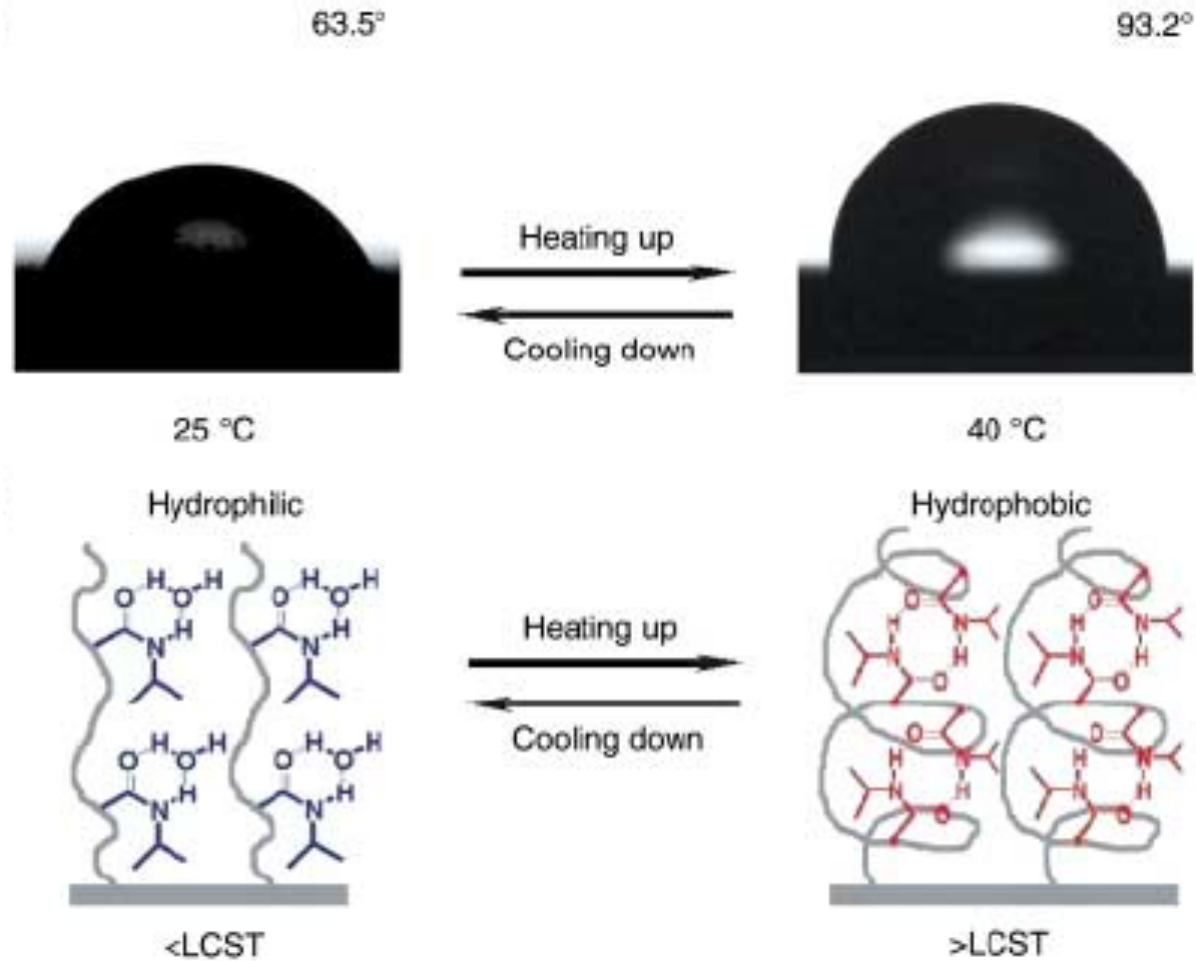


Change Potential

Lahann, J., *et al.*, *Science*. 2003, 299, 371.

Controlling Wettability

surface of poly(N-isopropylacrylamide)



Sun, T., *et.al.*, *Angew. Chem.* **2004**, 116, 361.

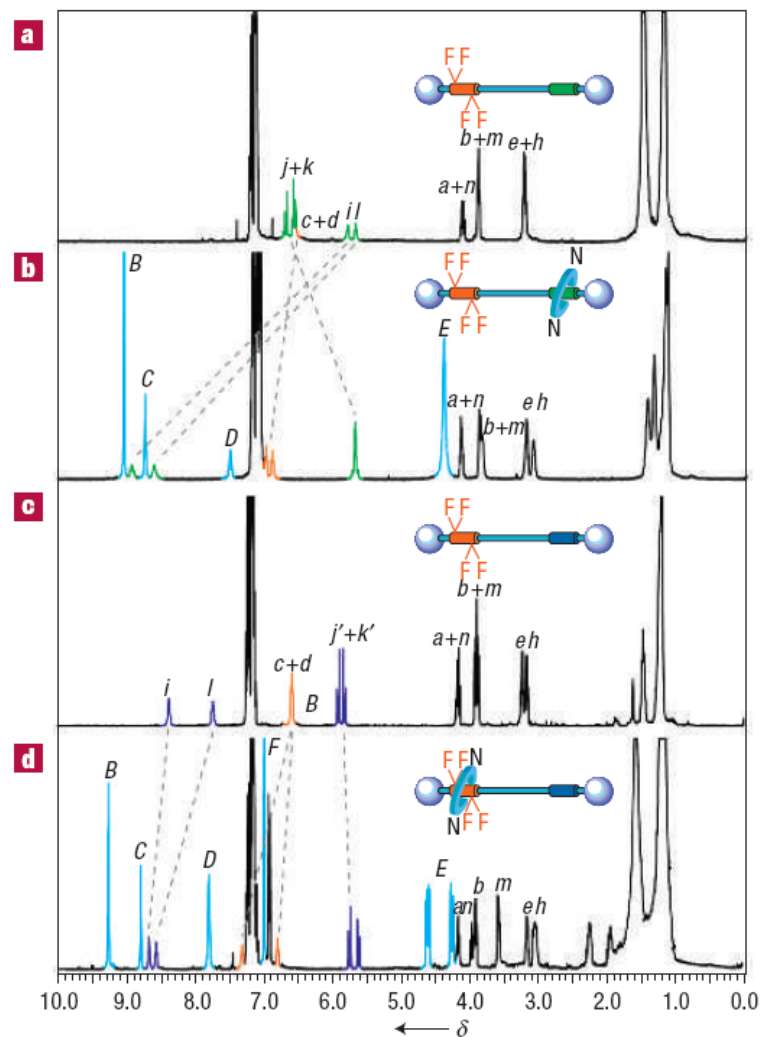
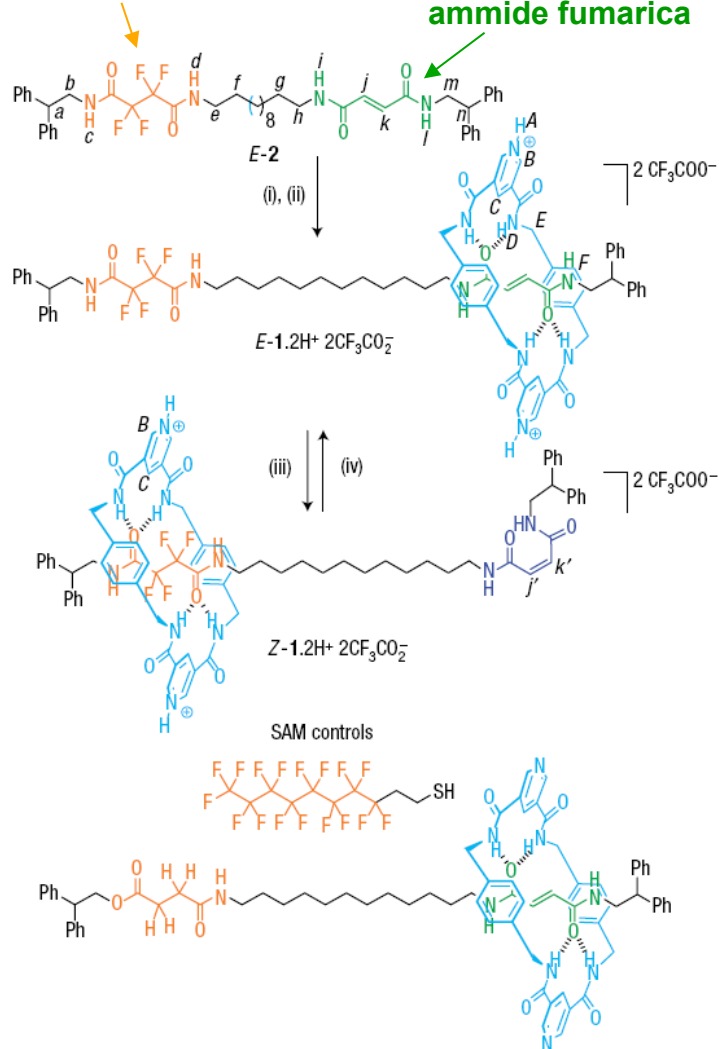
Macroscopic transport by synthetic molecular machines

nature materials VOL 4 SEPTEMBER 2005, 704

JOSÉ BERNÁ¹, DAVID A. LEIGH^{1*}, MONIKA LUBOMSKA², SANDRA M. MENDOZA², EMILIO M. PÉREZ¹,
 PETRA RUDOLF^{2*}, GILBERTO TEOBALDI³ AND FRANCESCO ZERBETTO^{3*}

tetrafluorosuccinamide

amide fumarica



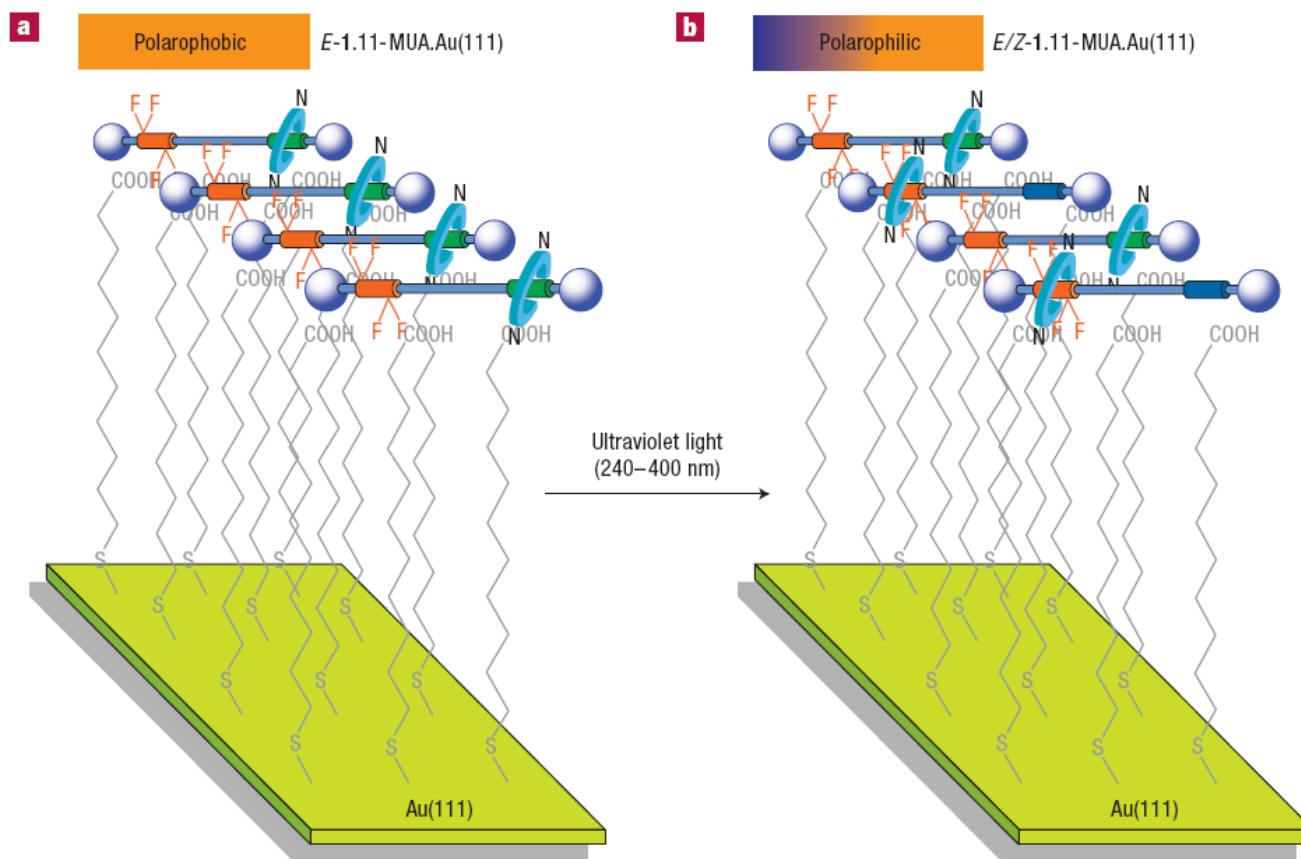


Figure 4 A photo-responsive surface based on switchable fluorinated molecular shuttles. a, Light-switchable rotaxanes with the fluoroalkane region (orange) exposed (*E*-1) were physisorbed onto a SAM of 11-MUA on Au(111) deposited on either glass or mica to create a polarophobic surface, *E*-1.11-MUA.Au(111). **b,** Illumination with 240–400 nm light isomerizes some of the *E* olefins to *Z* (giving a 50:50 ratio at the photostationary state if the reaction on the surface mirrors that in solution), causing a nanometre displacement of the rotaxane threads in the *Z*-shuttles which encapsulates the fluoroalkane units leaving a more polarophilic surface, *E/Z*-1.11-MUA.Au(111). Photoemission spectroscopy data are consistent with the molecular shuttles lying parallel to the Au surface (but they are not directionally aligned or necessarily linear as depicted for clarity in this cartoon).

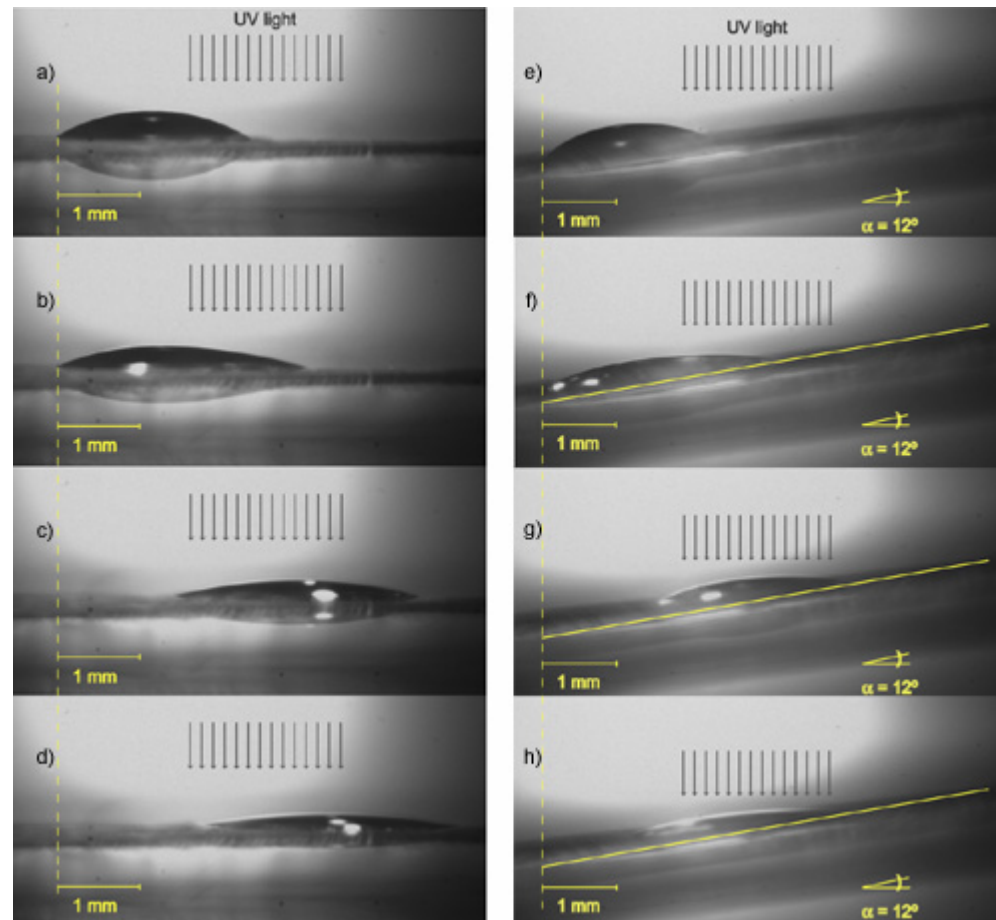


Figure 2. Light-driven directional transport of a 1.25 μl diiodomethane drop across the surface of monolayer of molecular machines, both flat (a)-(d) and up a twelve degree incline (e)-(h). This extrapolation across 6 orders of magnitude in length scales from mechanical motion at the molecular level to macroscopic transport is truly remarkable - the equivalent of millimetre motion of components in a machine working to raise an object to over twice the height of the CN Tower, the world's tallest building. The work done by the monolayer of molecular machines is stored as potential energy.

2D-SAMs

reactivity on surfaces

- effect of chain organization: esters at the end of long chains are hydrolyzed faster than esters at the end of shorter chains but slower than similar esters in solutions.
- lateral steric effect
- position of reactive sites
- partitioning of reactants in the organic interface

2D-SAMs

noncovalent modifications

- non specific adsorption of molecules
 - van der Waals and electrostatic forces
 - hydrophobic SAMs (formed from alkanethiols) adsorb proteins
- fusion of vesicles
 - hydrophilic functional groups (i.e. OH) promote the adsorption and rupture of vesicles.
 - hydrophobic SAMs (i.e. alkyl groups) promote the formation of hybrid bilayers that are excellent dielectric barriers. These structures provide a useful model system for studying the structure and function of cell membranes.
- selective deposition onto SAMs
 - pH control
- modifications via molecular recognition - multivalency
 - functional groups that bind through a network of hydrogen bonds, metal-ligand interactions, electrostatic interactions, or hydrophobic interactions – this modification is reversible

2D-SAMs

model bioassay

